

---

This is an electronic reprint of the original article.  
This reprint may differ from the original in pagination and typographic detail.

Khalid, Muhammad Kamran ; Agarwal, Vivek; Wilson, Benjamin P.; Takaluoma, Esther;  
Lundström, Mari

## **Applicability of solid process residues as sorbents for the treatment of industrial wastewaters**

*Published in:*  
Journal of Cleaner Production

*DOI:*  
[10.1016/j.jclepro.2019.118951](https://doi.org/10.1016/j.jclepro.2019.118951)

Published: 10/02/2020

*Document Version*  
Peer-reviewed accepted author manuscript, also known as Final accepted manuscript or Post-print

*Published under the following license:*  
CC BY-NC-ND

*Please cite the original version:*  
Khalid, M. K., Agarwal, V., Wilson, B. P., Takaluoma, E., & Lundström, M. (2020). Applicability of solid process residues as sorbents for the treatment of industrial wastewaters. *Journal of Cleaner Production*, 246, Article 118951. <https://doi.org/10.1016/j.jclepro.2019.118951>

---

This material is protected by copyright and other intellectual property rights, and duplication or sale of all or part of any of the repository collections is not permitted, except that material may be duplicated by you for your research use or educational purposes in electronic or print form. You must obtain permission for any other use. Electronic or print copies may not be offered, whether for sale or otherwise to anyone who is not an authorised user.

# Recovery and separation of rare earths and boron from spent Nd-Fe-B magnets

Fupeng Liu<sup>1,2</sup>, Antti Porvali<sup>2</sup>, JinLiang Wang<sup>1</sup>, Houqing Wang<sup>1</sup>, Chao Peng<sup>2</sup>, Benjamin P. Wilson<sup>2</sup>, Mari Lundström<sup>2</sup>

<sup>1</sup> Institute of Engineering Research, Jiangxi University of Science and Technology, Ganzhou, 341000, China.

<sup>2</sup> Hydrometallurgy and Corrosion, Department of Chemical and Metallurgical Engineering (CMET), School of Chemical Engineering, Aalto University, P.O. Box 12200, FI-00076 AALTO, Finland.

## Abstract:

The environmental and economic benefits of recycling spent Nd-Fe-B magnets are becoming increasingly important. Nevertheless, the reprocessing of this type of material by **conventional** processes remains a challenge due to the difficulties of rare earth elements (REEs) and Fe separation, low products purity and large-scale generation of boron wastewater. This research presents an effective approach for the comprehensive recovery of REEs, iron and boron from Nd-Fe-B magnet wastes. Investigations of the initial roasting pretreatment showed it to be an effective method that aids the subsequent selective separation of REEs, with the most suitable temperature determined to be 800 °C. During the following selective hydrochloric acid pressure leaching of the roasted magnet, the addition of 2 g/L NaNO<sub>3</sub> was found to significantly improve the separation of REEs and B from Fe. The results indicated that almost 99% of REEs and 97% of B could be extracted, whilst in contrast, less than 0.1% of iron dissolved, to leave a hematite rich residue. The extracted REEs were then directly precipitated as oxalates with >99% extraction and 99.95% purity at a value  $n(\text{oxalic acid})/n(\text{REEs})$  of 1, resulting in significant improvements to oxalic acid consumption and REEs product purity. In the final step, 99.5% of boron was recovered via a three-stage counter current extraction with 30% (v/v) (EHD) and 70% (v/v) sulfonated kerosene. These findings demonstrate that high recoveries of REEs, Fe and B are achievable with hydrochloric acid pressure leaching followed oxalate precipitation and boron recovery.

**Keywords:** Spent Nd-Fe-B magnets; Pressure leaching; Rare earth; Boron; Hematite

## 1. Introduction

Rare earth elements (REEs) are important strategic resources due to their unique properties and have been extensively used in a variety of high-technology fields, such as high-temperature superconductors, NiMH batteries, fluorescent lamps, permanent magnets

1 and catalysts (Jha et al., 2016; Petranikova et al., 2017; Hoogerstraete et al., 2014; Binnemans  
2 and Jones, 2014; Panayotova and Panayotov, 2012). Annually, almost 22% (>26 000 tons) of  
3 all REEs produced worldwide are utilized in the production of Nd-Fe-B magnets. Such  
4 magnets form the largest application among REEs (Nd, Pr, Gd, Dy and Ho) - both in terms  
5 of tonnage and market value - and it has been estimated that total Nd-Fe-B magnets  
6 production will reach 120,000 tons by 2020 (Yang et al. 2017; Benecki et al., 2011). The  
7 maximum lifetime of a Nd-Fe-B permanent magnet depends on its application and can range  
8 from just 2 - 3 years in the case of consumer electronics to 20 - 30 years for wind turbines  
9 (Du and Graedel, 2011; Yang et al., 2017; Tunsu, 2018). This has led to significant and  
10 increasing quantities of Nd-Fe-B magnet waste being generated both as a result of production  
11 – approx. 20 - 30% of the alloy is turned to scrap during processing – and disposal of  
12 permanent magnets at the end of their useful service life (Horikawa et al., 2006; Kumari et al.,  
13 2018). Recycling of the spent magnets is attractive since the material comprises of 30 - 40%  
14 REEs (Önal et al., 2017), however, global commercial recycling rates of end-of-life REEs  
15 products is currently estimated to be < 1% (Binnemans et al., 2015; Tunsu, 2018).  
16 Consequently, there is a need to develop new processes for the effective recycling of these  
17 spent magnets that not only provide environmental benefits but also are economically viable  
18 on an industrial scale.

19  
20  
21  
22  
23  
24  
25  
26  
27  
28  
29  
30  
31  
32  
33 In addition to the REEs, the other predominant metal in spent magnets is iron that  
34 comprises *ca.* 50 - 70% of the total mass and as a result, any recovery methodology must be  
35 able to separate effectively REEs from Fe (Venkatesan et al., 2018). Although some  
36 pyrometallurgical processes like liquid metal extraction (Sun et al., 2015), selective  
37 chlorination (Itoh et al., 2008), glass slag method (Saito et al., 2003), chemical vapor  
38 transport (Murase et al., 1995) and sulfate or nitrate selective roasting (Önal et al., 2015; Önal  
39 et al., 2017) have been developed to separate REEs and Fe, some of these pyrometallurgical  
40 methods are highly energy intensive, low recovery efficiencies of REEs and may also result  
41 in secondary environmental pollution. In contrast, hydrometallurgical approaches can offer an  
42 alternative that allows high purity REEs products to be obtained with lower levels of  
43 associated air pollution (Kumari et al., 2018; Jha et al., 2018). For example, in the early  
44 1990s, Lyman and Palmer (1993) developed a method that utilizes sulfuric acid leaching  
45 followed by sulfate double salt precipitation, which results in almost 98% of REEs being  
46 extracted with 2 mol/L H<sub>2</sub>SO<sub>4</sub> and L/S ratio of 10 at ambient temperature. Nevertheless, REE  
47 solution enrichment to high concentrations is not possible due to the low solubility of REE  
48 sulfates, whereas some heavy REEs like Dy and Ho are lost due to their incomplete  
49  
50  
51  
52  
53  
54  
55  
56  
57  
58  
59  
60  
61  
62  
63  
64  
65

1 precipitation by the double sulfate precipitation process (Beltrami et al., 2015; Battsengel et  
2 al., 2018).

3  
4 Several efforts have been made to eliminate the negative influence of sulfate ion by the use  
5 of alternative leaching systems based on nitric, hydrochloric and acetic acids. The results  
6 showed that high levels (>95%) of both REEs and Fe were leached due to the higher  
7 solubility of REEs in chloride and nitrate media (Lee et al., 2013; Önal et al., 2017). The  
8 main drawbacks to these methods is that the presence of large amounts of dissolved iron not  
9 only hinders REEs oxalate precipitation, - a typical industrial process for REEs separation -  
10 but also makes the subsequent purification more complex, resulting in increased costs and  
11 low-value products such as Fe(OH)<sub>3</sub>, and Fe/Co containing REEs oxalates (Bandara et al.,  
12 2016; Venkatesan et al., 2018). As a result, alternative methods of selective leaching  
13 processes have been developed to overcome the disadvantages of complete leaching. Rabatho  
14 et al. (2013) studied a leaching system composed of a 1mol/L HNO<sub>3</sub> and 0.3 mol/L H<sub>2</sub>O<sub>2</sub>  
15 mixture, which could dissolve 70 -90% of REEs and <15% of Fe from spent magnet in 5 min  
16 at 80 °C. Nonetheless, 20 - 30% losses of Nd and Dy were observed during the iron removal  
17 step, whereas the use of HNO<sub>3</sub> and H<sub>2</sub>O<sub>2</sub> significantly increases the operational cost.

18  
19 Another alternative method that has been widely adopted for REEs recovery is the  
20 oxidative roasting – selective leaching process (Koyama et al., 2009; Lee et al., 1998;  
21 Hoogerstraete et al., 2014; Kumari et al., 2018). In this process, accurate control of the  
22 roasting is essential as insufficient oxidation of the Nd<sub>2</sub>Fe<sub>14</sub>B causes some of iron to dissolve  
23 into the solution as ferrous ion, the pH stability of which subsequently inhibits the selective  
24 leaching of REEs. On the other hand, excessive roasting leads to the formation of partial  
25 insoluble ferrites like NdFeO<sub>3</sub> that also make high recovery efficiencies of REEs a challenge  
26 (Lee et al., 1998; Önal et al., 2015; Firdaus et al., 2018). In order to decrease the roasting  
27 temperature, thereby avoiding the formation of NdFeO<sub>3</sub>, the pretreatment of NaOH grinding  
28 methods was also adopted to firstly achieve the transformation of REEs from its alloys to  
29 hydroxides (Yoon et al., 2015).

30  
31 After roasting, low concentration hydrochloric acid leaching process was conventional and  
32 economic process for the recovery of REEs from roasted magnet wastes. Hoogerstraete et al.  
33 (2014) found that almost all the iron remains in the leach residue if the molar ratio of HCl and  
34 REEs is optimized. However, the complete separation of REEs and iron could only be  
35 achieved after 15 h with a  $n(\text{HCl})/n(\text{REEs})$  ratio of 3.5 at 80 °C, and the dissolved iron in the  
36 leachate was mainly precipitated as Fe(OH)<sub>3</sub> or FeOOH (at pH >1.5). Kumari et al. (2018)  
37 found that the leaching kinetics are controlled by both diffusion through the solution  
38  
39  
40  
41  
42  
43  
44  
45  
46  
47  
48  
49  
50  
51  
52  
53  
54  
55  
56  
57  
58  
59  
60  
61  
62  
63  
64  
65

1 boundary layer and the chemical reaction at the interface, therefore both longer reaction  
2 duration and increased temperature can enhance REEs leaching. In addition, Koyama et al.  
3 (2009) found that more than 99% of the REEs content of Nd-Fe-B spent magnets could be  
4 dissolved in 0.02 mol/L HCl with an industrially irrelevant low L/S (mL/g) ratio of 1000 ( $T =$   
5  $180\text{ }^{\circ}\text{C}$ ,  $t = 2\text{h}$ ) with  $< 0.5\%$  of related Fe dissolution.  
6  
7

8  
9 The advantage of pressure leaching is that the iron mainly exists in the leaching residue as  
10 hematite ( $\text{Fe}_2\text{O}_3$ ), which - when compared to ferrihydrite  $\text{Fe}(\text{OH})_3$ , akaganeite ( $\text{FeOOH}$ ) and  
11 jarosite ( $\text{MFe}_3(\text{SO}_4)_2(\text{OH})_6$  - has some significant advantages like good environmental  
12 stability, low cation adsorption capacity and potential marketability to the steel industry  
13 (Riveros and Dutrizac, 1997). The drawback of the method outlined by Koyama et al. (2009)  
14 is that a high liquid-solid ratio makes the subsequent enrichment and recovery of REEs from  
15 very dilute solutions problematic. In addition, as the application range of the process is  
16 narrow, it is difficult to achieve selective separation of iron for materials that are not fully  
17 oxidized due to the sluggish oxidation kinetics of Fe(II) in the acidic leachate ( $\text{pH} < 4$ )  
18 (Morgan and Lahav, 2007). Although the introduction of  $\text{H}_2\text{O}_2$  can obviously promote the  
19 iron removal in the pressure leaching (Langová and Matýšek, 2010), the consumption of  
20  $\text{H}_2\text{O}_2$  is large because of the thermolabile nature of  $\text{H}_2\text{O}_2$  (Liu et al., 2017).  
21  
22

23  
24 Another challenge in the recycling of spent Nd-Fe-B magnets is the removal of boron.  
25 Currently, most research focuses on the recovery of valuable metals such as REEs, Co and Fe,  
26 although there are a few reports on boron retrieval from spent magnet waste (Tunsu, 2018;  
27 Jha et al., 2018). Nevertheless, the ability to reclaim also boron is necessary in order to avoid  
28 its accumulation into products or wastewaters during the recycling process. Additionally, the  
29 recovery of boron can allow its circulation either back to the industrial manufacture of  
30 permanent magnets or other uses like the production of fiberglass, detergents, fertilizers, etc.  
31 (Tagliabue et al., 2014; Wolska and Brijak, 2013). Although adsorption separation and  
32 membrane filtration processes have been widely applied to boron recovery from low  
33 concentration boron solutions such as desalinate seawater and salt lake brine (Sasaki et al.,  
34 2013; Tu et al., 2010; Xu et al., 2008), these methods are not suitable for acidic solutions  
35 containing high concentrations of B.  
36  
37

38  
39 In the current study, a new pressure leaching approach for Nd-Fe-B magnets is taken by  
40 introducing  $\text{NaNO}_3$  as the oxidant. By this method, the separation between REEs and Fe  
41 leaching could be significantly improved. In order to present a complete process scheme for  
42 spent Nd-Fe-B magnets, the current work investigates not only the selective pressure acid  
43 leaching process, but also the subsequent REEs oxalates recovery and boron removal by a 2-  
44  
45  
46  
47  
48  
49  
50  
51  
52  
53  
54  
55  
56  
57  
58  
59  
60  
61  
62  
63  
64  
65

ethyl-1,3-hexanediol/sulfonated kerosene solvent combination, with the focus on behavior of impurities and valuable metals during each process step.

## 2. Experimental

### 2.1. Experimental procedure

#### 2.1.1. Pretreatment and pressure leaching

Spent Nd-Fe-B magnets, obtained from a company in Finland, were firstly demagnetized in a muffle furnace (air atmosphere) by heating at 350 °C for 1h, before being crushed and ground in a mill (Pulverisette 9, Fritsch, Germany). It need to be noted that as the particle size of magnet waste decreases the waste will become pyrophoric in character, readily reacting with the heat of the milling and oxygen present in the air (Kruse et al., 2017). Once ground, the sample was further roasted in the air at different temperatures (700 °C; 800 °C; 900 °C) for 2h. The pressure acid leaching test was performed by mixing the roasted spent magnet and hydrochloric acid solution at a pre-determined L/S ratio in a 1 L titanium autoclave with agitator speed 300 r/min. The temperature and pressure range were listed in the Table 1. After filtration, the leach residue was washed with deionized water and both the residue and filtrate samples were analyzed. The leaching efficiency (%E) is defined as:

$$\%E = (C_M \times V)/(m \times w_M) \times 100\% \quad (1)$$

Where  $C_M$  is the concentration of metals in the leachate (g/L);  $V$  is the volume of leachate (L);  $m$  is the mass of input spent NdFeB magnet (g) and  $w_M$  is the amount of an element in the roasted magnet.

#### 2.1.2. REEs oxalate precipitation

In order to investigate the REEs oxalates precipitation phenomena, the effect of ferrous and ferric ion on the recovery and purity of REEs oxalate was investigated by a synthetic solution with  $[Nd^{3+}] = 20$  g/L and different concentrations of ferrous ions and ferric ions. Then, the oxalic acid was directly added into the simulated solution with  $n(\text{oxalic acid})/n(\text{REEs})$  of 1.5 ( $t = 1\text{h}$ ,  $T = 50$  °C). In addition, the consumption of oxalic acid in high concentration iron (10 g/L) solution and Fe-free solution was investigated under the same experimental conditions. Afterwards, the resultant precipitate was filtered, washed with

1 distilled water before being dried at 100 °C. The precipitation of REEs (%P) was calculated  
2 as follows:  
3  
4

$$5 \quad \%P = (1 - C_1/C_0) \times 100\% \quad (2)$$

6  
7  
8

9 Where  $C_0$  and  $C_1$  represent the initial and final concentration of REEs before and after  
10 precipitation procedure, respectively.  
11  
12

### 13 **2.1.3. Boron solvent extraction**

14 After the REEs precipitation, dissolved boron was extracted and enriched by solvent  
15 extraction. The extraction experiments were carried out in 125 mL separation funnels by  
16 mixing an organic phase and the aqueous solution, with different organic/aqueous phase (O/A)  
17 ratios, at 30 °C for 10 min in an incubator shaker (Model KS 3000i, IKA, Germany) . The  
18 organic phase consisted of 30% (v/v) 2-ethyl-1,3-hexanediol and 70% (v/v) sulfonated  
19 kerosene (both provided by Shanghai Rare-earth Chemical Co., Ltd., China) as the solvent  
20 for extraction. The loaded organic phase was subsequently stripped with 0.1 mol/L NaOH for  
21 15 min at an O/A ratio of 1:2 and 30 °C.  
22  
23  
24  
25  
26  
27  
28  
29  
30

31 The investigated parameters utilized at each processing stage are displayed in Table 1. All  
32 chemical reagents utilized were of analytical grade and deionized water was used throughout  
33 the experiments for the solution preparation.  
34  
35  
36  
37

38 Table 1. Main parameters investigated during the experiments.  
39

40 Experiments	41 Investigated Parameters
42 Oxidative Roasting	43 Temperature: 600-900 °C; Roasting time: 120 min;
44 Pressure Leaching	45 Liquid-to-solid (L/S): 4-12 ml/g; Temperature: 100-200 °C; HCl: 46 0.2-0.8 mol/L; Reaction time: 20-180 min; NaNO <sub>3</sub> : 0-2 mg/L 47 48
49 Oxalate Precipitation	50 Temperature: 25-50 °C; $n(\text{oxalic acid})/n(\text{REEs})$ : 0.8-1.2; Reaction 51 time: 10-180 min; Fe <sup>3+</sup> : 0-15 g/L 52
53 Boron 54 Solvent Extraction	55 Reaction time: 5–15 min; temperature: 30 °C; N235(v/v): 5–10%; 56 organic/aqueous phase ratio (v/v) (O:A): 2:1–1:6 57

## 58 **2.2. Analytical methods**

59  
60  
61  
62  
63  
64  
65

1 The chemical analysis of the spent magnet, leaching residues and products formed were  
2 performed using a number of different spectroscopic techniques. Firstly, the solid samples  
3 were subjected to total dissolution in aqua regia, then the resultant solution concentrations of  
4 REEs, Fe, Co, B and other impurities were determined by inductively coupled plasma-optical  
5 emission spectroscopy (ICP-OES, Perkin Elmer Optima 7100 DV, USA). The Fe(II)  
6 concentrations in the spent magnet and leaching residues were analyzed by the chemical  
7 dissolution - potassium dichromate method. In contrast, the Fe(III) concentrations in leachate  
8 were analyzed by a precipitation separation - EDTA titration method (Liu et al, 2017). EPMA  
9 - Electron-Probe X-ray Microanalysis, of the Fe and REEs (Nd, Pr, Gd, Dy and Ho)  
10 distribution behaviors were measured by a JEOL JXA-8230 instrument operated at 15 kV  
11 with a 10 nA beam current. The main mineral phases within the samples were identified by  
12 XRD (PANalytical X'Pert Pro Powder, Almelo, the Netherlands) using a  $\text{CoK}\alpha$  radiation  
13 source with a 40 kV acceleration potential and current of 40 mA. XRD diffractograms were  
14 analyzed by using HighScore 4.0 Plus software. The morphology and size of the REEs  
15 products were determined by SEM (A LEO 1450, Carl Zeiss Microscopy GmbH, Jena,  
16 Germany). All the other chemicals used in the leaching, precipitation and solvent extraction  
17 were of analytical grade.

### 3. Results and discussion

#### 3.1. Spent NdFeB magnet pretreatment

36 After demagnetization, crushing and grinding, ca. 80% of the particles in the spent magnet  
37 powder were  $<160\ \mu\text{m}$ . Fig. 1 shows the EPMA results for distributions of Fe, Dy, Gd, Ho,  
38 Nd and Pr in the material. The results indicate that most of rare earth elements mainly co-  
39 exist with Fe, but also that some REEs like Nd, Gd and Pr have their own independent phase.  
40 These independent phases are akin to inclusions within the Fe matrix, which necessitate very  
41 fine grinding to ensure the best recovery of the REEs.

42 After grinding, oxidation roasting with different temperatures (700 °C, 800 °C and 900 °C)  
43 was undertaken, and the roasting time was 2 h. XRD results, shown in Fig. 2, indicate that the  
44 roasting temperature of 700 °C led to the incomplete oxidation of both the Fe and REEs in  
45 the spent magnet as  $\text{Nd}_2\text{Fe}_{14}\text{B}$  diffraction peaks are still present. The presence of unoxidized  
46 Fe leads to problems in the subsequent process steps as it will dissolve during leaching and  
47 remain in the solution as  $\text{Fe}^{2+}$  up to pH value of 6-8. In contrast at  $T = 900\ \text{°C}$ ,  $\text{NdFeO}_3$  is  
48 clearly formed, which significantly suppresses the leaching of REEs. Consequently, a too  
49  
50  
51  
52  
53  
54  
55  
56  
57  
58  
59  
60  
61  
62  
63  
64  
65

high oxidation temperature will result in poor REEs extraction, whereas insufficient roasting will cause poor selectivity due to  $Fe^{2+}$  dissolution. Based on the roasting results, 800 °C was selected as the most suitable roasting temperature. The contents of REEs, Fe and other main elements of interest found in the spent magnet powder before and after roasting at 800 °C are shown in Table 1. As it can be seen, the content of Fe decreased from 62.7 to 46.4% before and after roasting, which indicates a net mass gain by 35.1% for the sample. REEs including Nd, Pr, Dy, Gd and Ho accounted for 25.8% of the total elements, whereas the B and Co content were both >0.6%.

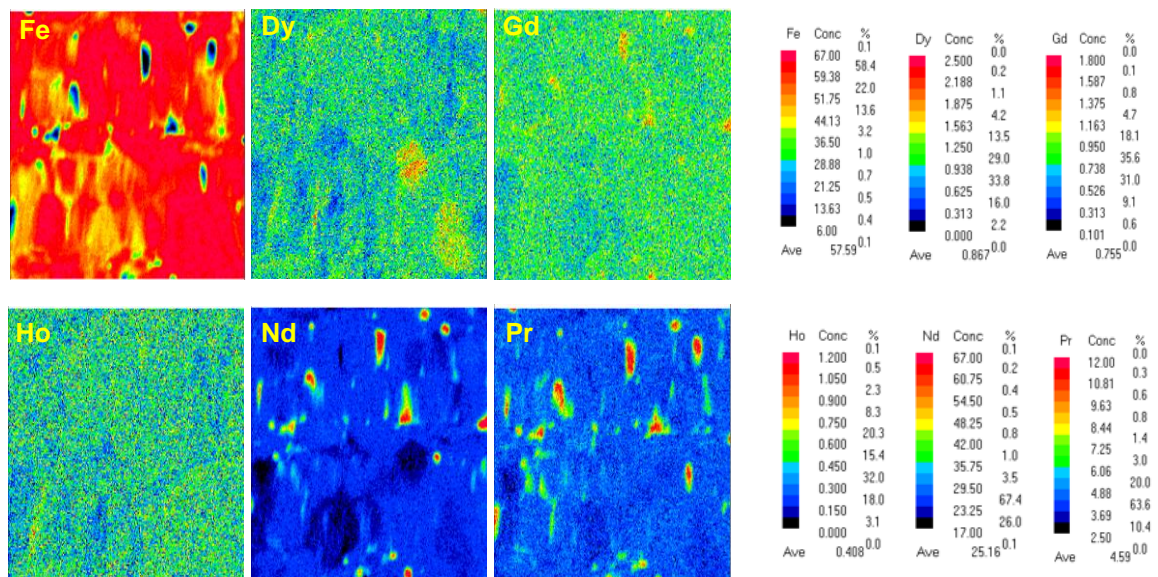


Fig. 1. EPMA distribution maps of Fe, Pr, Nd, Dy, Gd and Ho in the spent magnet powder.

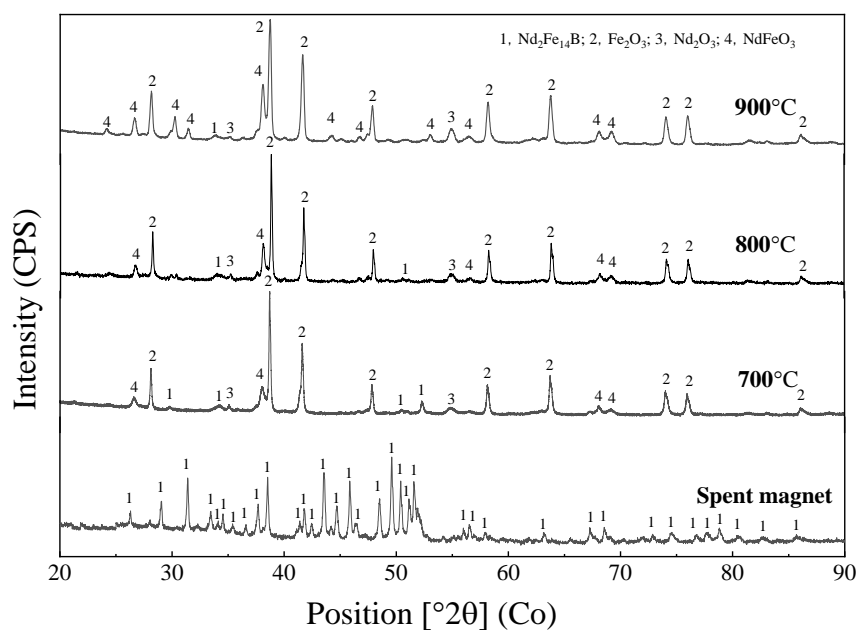


Fig. 2. XRD pattern of the spent Nd-Fe-B magnet powder before and after roasting.

Table 1. Chemical composition of spent Nd-Fe-B magnet powder before and after roasting

Elements	Fe	Nd	Pr	Dy	Gd	Ho	B	Co
Before (wt. %)	62.67	25.81	6.10	1.80	0.19	0.84	0.96	0.87
After (wt. %)	46.38	19.19	4.55	1.33	0.14	0.62	0.71	0.64

### 3.2. REEs oxalate precipitation in high concentration iron solution

From the analysis of the raw materials, it was found that the iron content was as high as 50%, which in the traditional hydrochloric acid leaching or sulfuric acid leaching of magnet waste makes the leaching of Fe inevitable. In order to determine the effect of Fe on the REEs oxalate precipitation behavior, the REEs oxalate precipitation was investigated in synthetic solution at different concentrations of the ferrous and ferric ion. The purity of the precipitate was found to increase from 98.5% to 99.9% as the proportion of ferric ion increases from zero to 100% (Fig. 3). However, the associated precipitation efficiencies of the REEs decreased significantly from 98.6% to 76.0%. It is clear that the presence of Fe(II) in the oxalate solution had a negative impact on the purity of REEs products and that ferric ions

1  
2  
3  
4  
5  
6  
7  
8  
9  
10  
11  
12  
13  
14  
15  
16  
17  
18  
19  
20  
21  
22  
23  
24  
25  
26  
27  
28  
29  
30  
31  
32  
33  
34  
35  
36  
37  
38  
39  
40  
41  
42  
43  
44  
45  
46  
47  
48  
49  
50  
51  
52  
53  
54  
55  
56  
57  
58  
59  
60  
61  
62  
63  
64  
65

result in a substantial increase in oxalic acid consumption, due to the strong complexation of oxalate anion with ferric cation (Liu et al., 2017).

Fig. 4 shows that the REEs precipitation is above 99.0% when the value of  $n(\text{oxalic acid})/n(\text{REEs})$  reaches 3.0. This means that there are still notable amounts of dissolved oxalic acid present that results in oxalate accumulation within the aqueous phase. Evidently, a low concentration of Fe in solution is beneficial for the process, as it enhances REEs recovery and minimizes the oxalate accumulation in the pregnant leach solution (PLS). In the current work, a strategy of minimal Fe dissolution was achieved by adopting a high pressure leaching process for the roasted spent magnet material, which allows to convert the dissolved iron into hematite prior to the REEs oxalate precipitation stage.

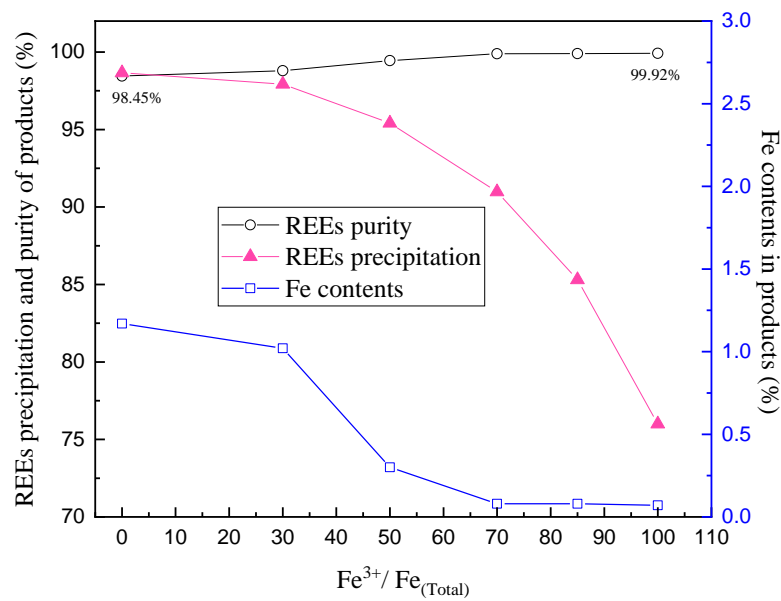


Fig. 3. Effect of  $\text{Fe}^{3+}$  ion on the REEs precipitation and purity of oxalate products ( $T = 50\text{ }^{\circ}\text{C}$ ;  $t = 60\text{ min}$ ;  $n(\text{oxalic acid})/n(\text{REEs}) = 1.8$ ;  $\text{Nd}^{3+} = 20\text{ g/L}$ ;  $\text{Fe}_{(\text{total})} = 10\text{ g/L}$ ;  $\text{pH} = 0.86$ ).

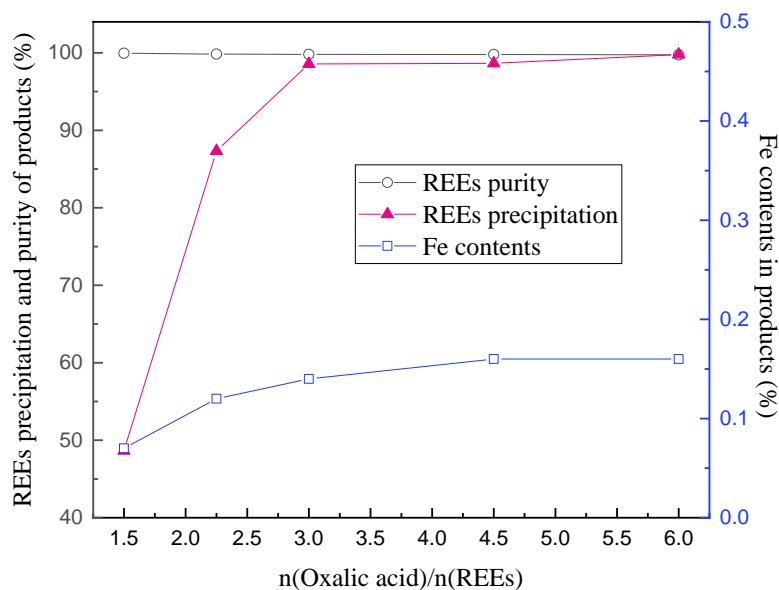


Fig. 4. Effect of oxalic acid on the REEs precipitation and purity of oxalate products ( $T = 50\text{ }^{\circ}\text{C}$ ;  $t = 60\text{ min}$ ;  $\text{Nd}^{3+} = 20\text{ g/L}$ ;  $\text{Fe}^{3+} = 10\text{g/L}$ ;  $\text{pH} = 0.79$ ).

### 3.3. Pressure acid leaching

#### 3.3.1 Effect of temperature

The effect of leaching temperature on the recovery of REEs (Nd, Pr, Gd, Ho and Dy), Fe, Co and B from roasted spent magnet powder was investigated with a solution containing 0.6 mol/L HCl. Results presented in Fig. 5 indicate that the leaching of REEs increased from 87.45% to 98.21% as the temperature increased from 120 °C to 180 °C, although a further increase in the temperature from 180 °C to 240 °C resulted in only minor changes in the extraction of REEs. The main reason for the increase is that some of the ferrites produced in roasting, like  $\text{NdFeO}_3$ , can dissolve at temperatures higher than 150 °C (Langová and Matýšek, 2010). XRD results (Fig. 6) show that no  $\text{NdFeO}_3$  could be identified in the leach residues at temperatures higher than 180 °C. Moreover, the same findings also indicate that the main Fe-containing phases are akaganeite ( $\text{FeOOH}$ ) and hematite ( $\text{Fe}_2\text{O}_3$ ) at 120 °C, but that almost all Fe is present as hematite after leaching at 180°C (Riveros and Dutrizac, 1997; Cudennec and Lecerf, 2006). This transformation from akaganeite to hematite can reduce the losses of REEs due to adsorption or co-precipitation, as demonstrated by the marked decrease from 8.45% to 3.65% of Fe leaching due to hematite precipitation as temperature increases from 120 °C to 240 °C. Under the same conditions, leaching of B and Co remained almost

constant at 96% and 9% over the whole temperature range investigated. The low recovery of cobalt is primarily attributed to the presence of insoluble cobalt ferrite ( $\text{CoFe}_2\text{O}_4$ ) produced in the roasting stage when the roasting temperature was above  $700\text{ }^\circ\text{C}$  (Radwan and El-Shobaky, 2000).

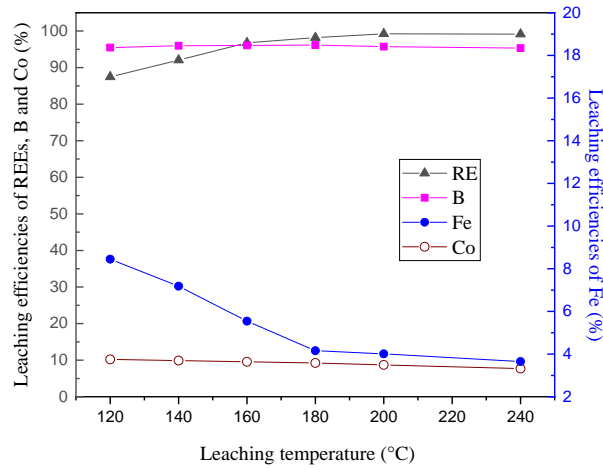


Fig. 5. Effect of leaching temperature on the leaching efficiencies of REEs, B, Fe and Co ( $\text{HCl} = 0.6\text{ mol/L}$ ;  $\text{NaNO}_3 = 0\text{ g/L}$ ;  $t = 120\text{ min}$ ;  $L/S = 10$ ).

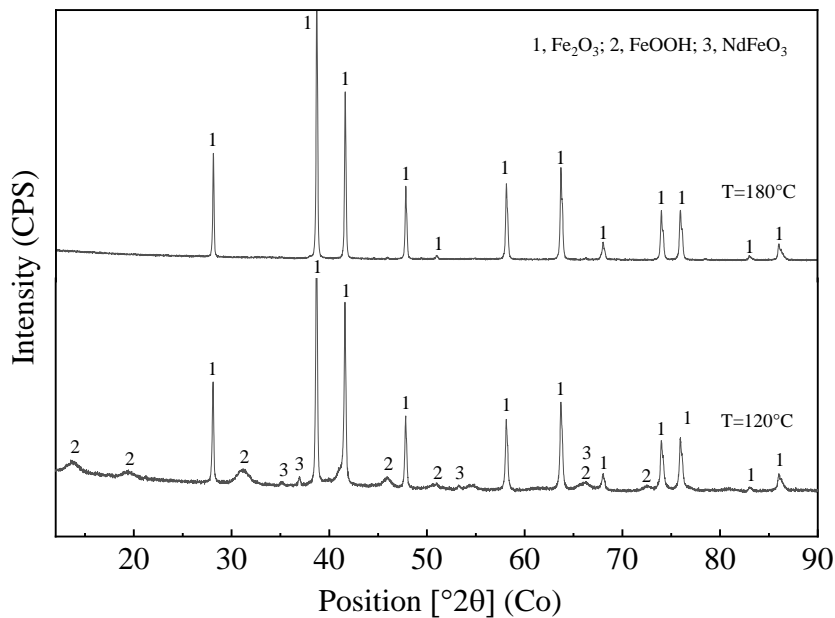


Fig. 6. X-ray diffraction patterns of the leach residues after leaching at  $T = 120$  and  $180\text{ }^\circ\text{C}$ .

### 3.3.2. Effect of leaching time

The effect of the leaching time on the leaching of REEs, B, Fe and Co is presented in Fig.

7. These results suggest that the leaching of REEs and B is rapid as approximately 90 % of the REEs and 75% of the B extracted within the first 30 min, whereas the highest leaching efficiencies (REEs = 98.2% and B = 96.1%) were reached after 2h. In contrast, although the leaching of Fe initial increases to 6.1% after 30 min, there is a gradual and continuous decrease over the remainder of the experiment. The reason for this observed decrease is ascribed to the increase in akaganeite (FeOOH) and hematite (Fe<sub>2</sub>O<sub>3</sub>) formation with prolonged time under high temperature and low acidity conditions. When compared with the metastable ferrihydrite Fe(OH)<sub>3</sub> and akaganeite (FeOOH), the hematite has good crystallization, poor cation adsorption properties and its solubility,  $K_{sp}$  of  $10^{-43}$  is lower than either ferrihydrite ( $10^{-39}$ ) or akaganeite ( $10^{-41}$ ) (Cudennec and Lecerf, 2006). Nonetheless, the transformation from ferrihydrite to hematite is slow, therefore extended leaching times support the complete removal of Fe, in order to enhance the selective leaching of REEs (Riveros and Dutrizac, 1997). Under the same conditions, the leaching of cobalt remained nearly constant at approximately 9% for all leaching times investigated due to the weak solubility of CoFe<sub>2</sub>O<sub>4</sub> in the low acid solution (Hubli et al., 1997; Tang et al., 2008).

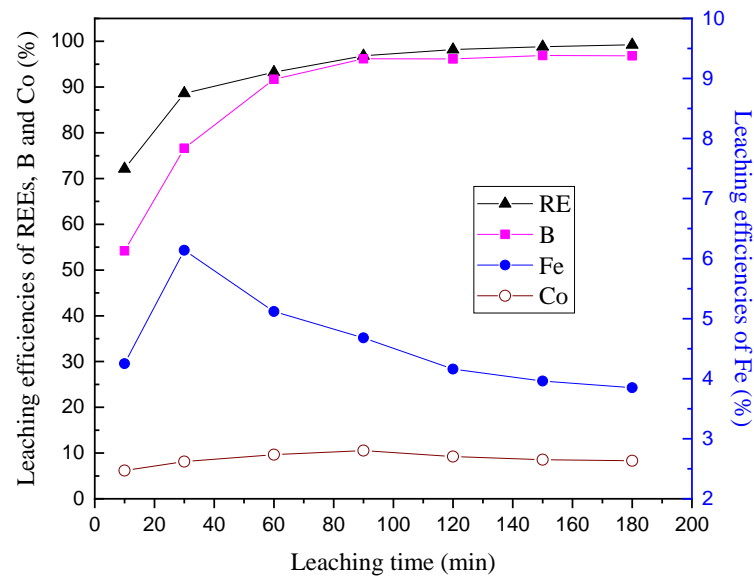
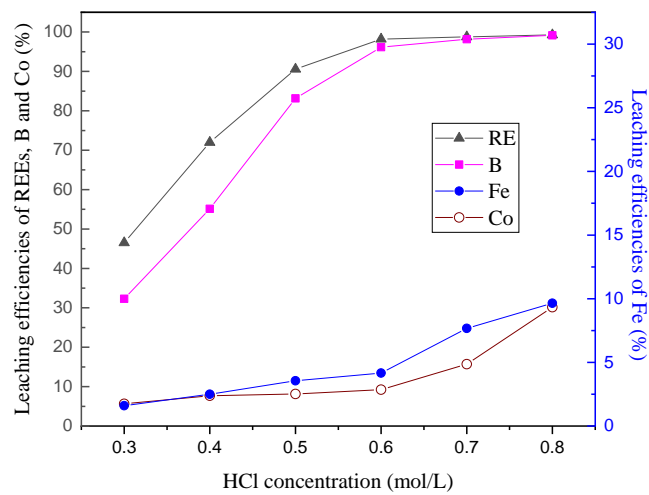


Fig. 7. Effect of leaching time on the leaching efficiencies of REEs, B, Fe and Co ( $T = 180\text{ }^{\circ}\text{C}$ ; HCl = 0.6 mol/L; L/S = 10; NaNO<sub>3</sub> = 0 g/L).

### 3.3.3. Effect of hydrochloric acid concentration

The effect of hydrochloric acid concentration on the leaching of REEs (Nd, Pr, Gd, Ho and Dy) and Fe was examined by varying the HCl concentration from 0.3 mol/L to 0.8 mol/L.

1 The results, shown in Fig. 8, indicate that the extraction of REEs and B increased  
 2 considerably as the hydrochloric acid concentration increased from 0.3 mol/L to 0.6 mol/L -  
 3 from 46.5 to 98.2% for REEs and from 32.3 to 96.1% for B, respectively. In contrast, further  
 4 increases in hydrochloric acid concentration from 0.6 mol/L to 0.8 mol/L, only resulted in a  
 5 minor change to the level of REEs and B extracted. Under the same conditions, the leaching  
 6 of Fe and Co increased significantly when the initial hydrochloric acid concentration  
 7 was >0.6 mol/L. The XRD results (Fig. 9) of leach residues showed that the REEs ferrite is  
 8 difficult to dissolve under low acidity conditions, which results in significantly lower levels  
 9 of REEs and Fe. Conversely, high levels of acidity facilitates the leaching of all the metals  
 10 from the roasted spent magnet. Irrespectively, the presence of dissolved Fe and Co consumes  
 11 some oxalic acid during the REEs oxalate precipitation and this can have an adverse effect on  
 12 the purity of the resultant REEs oxalates (Venkatesan et al., 2018).  
 13  
 14  
 15  
 16  
 17  
 18  
 19  
 20  
 21  
 22  
 23



24  
 25  
 26  
 27  
 28  
 29  
 30  
 31  
 32  
 33  
 34  
 35  
 36  
 37  
 38  
 39  
 40  
 41  
 42 Fig. 8. Effect of HCl on the leaching efficiencies of REEs, B, Fe and Co ( $T = 180^{\circ}\text{C}$ ;  $t = 120$   
 43 min;  $L/S = 10$ ;  $\text{NaNO}_3 = 0 \text{ g/L}$ ).  
 44  
 45  
 46  
 47  
 48  
 49  
 50  
 51  
 52  
 53  
 54  
 55  
 56  
 57  
 58  
 59  
 60  
 61  
 62  
 63  
 64  
 65

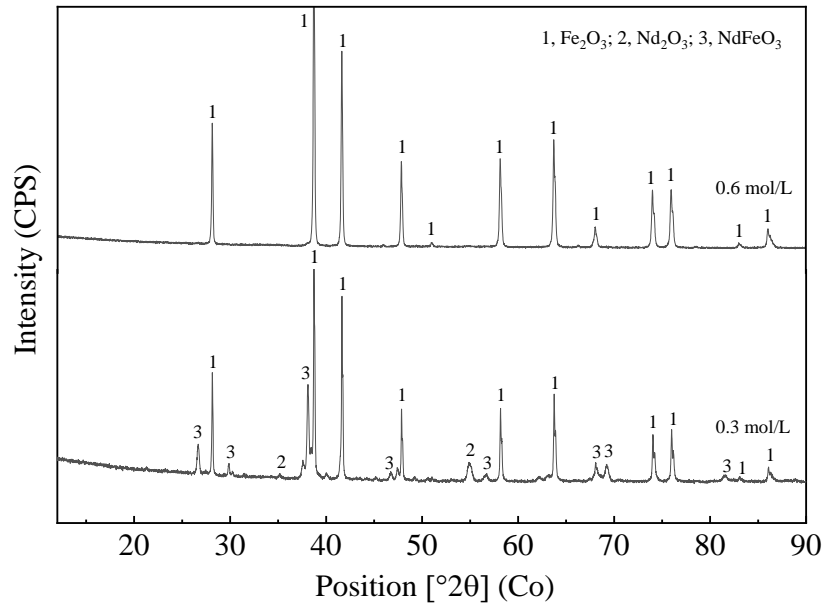


Fig. 9. X-ray diffraction patterns of the leach residues from different acid concentration.

### 3.3.4. Effect of L/S ratio

The leaching results of REEs, B, Fe and Co obtained at different liquid-to-solid (L/S) ratio are displayed in Fig. 10. These results indicate that the leaching of REEs and B increased substantially as L/S increased from 4 to 12, whereas the leaching of Fe remains low until the L/S ratio >10 at which point it starts to increase from 4 to 9%. The increase of Fe leaching results from the higher amount of acid available at the lower pulp density. This increases the Fe dissolution and delays  $Fe^{3+}$  hydrolysis, resulting in the formation of  $Fe_2O_3$  precipitate (Eq. (3)). On the other hand, the leaching of Co also increases gradually as the L/S ratio changes from 4 to 12, with approximately 11% of Co leached at a L/S ratio of 10. In order to achieve the selective separation of REEs and Fe, the optimum L/S ratio is 10, allowing high level of REEs (~98%) and B (~96%) leaching with minimal Co or Fe impurities.



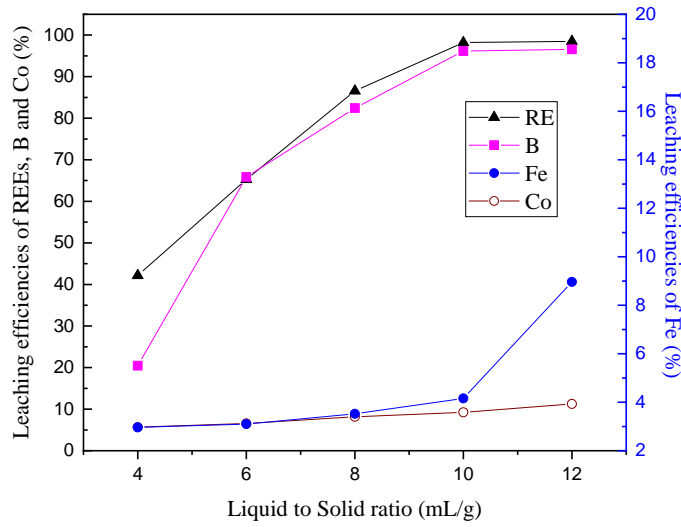
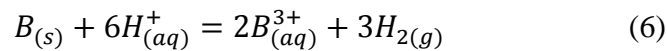
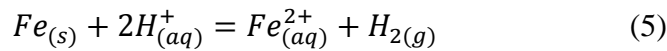


Fig. 10. Effect of liquid to solid (L/S) ratio on the leaching efficiencies of REEs, B, Fe and Co ( $T = 180\text{ }^{\circ}\text{C}$ ;  $\text{HCl} = 0.6\text{ mol/L}$ ;  $\text{NaNO}_3 = 0\text{ g/L}$ ;  $t = 120\text{ min}$ ).

### 3.3.5. Effect of $\text{NaNO}_3$ concentration

Phase analysis results of roasted spent magnet samples show that, in addition to the presence of  $\text{NdFeO}_3$ ,  $\text{Fe}_2\text{O}_3$  and  $\text{Nd}_2\text{O}_3$ , the  $\text{Nd}_2\text{Fe}_{14}\text{B}$  phase is still present within the materials due to incomplete oxidation of the material. As the REEs and Fe in this metallic alloy have high negative standard electrode potentials, they are easily dissolved by hydrochloric acid via the following reactions outlined in Eqs. (4) - (6):



After treatment with hydrochloric acid, ferrous ions predominate within the PLS. Fe(II) tends to be stable in solution up to a pH of 6 and Fe(II) oxalates are highly insoluble, whereas in contrast, Fe(III) precipitates at a pH around 2-3 and Fe(III) oxalates are highly soluble. Therefore, in order to achieve a good separation of REEs and Fe, the selective oxidation of Fe(II) is necessary and  $\text{NaNO}_3$  was selected as an oxidant in order to mitigate the iron dissolution.

The effect of sodium nitrate addition on the leaching of REEs, B, Fe and Co were examined with a total pressure 0.62 MPa, an HCl concentration of 0.6 mol/L and an L/S ratio

of 10 at 180 °C for 2 h (Fig. 11). As can be observed, the leaching of Fe shows a continuous decrease - from approx. 4% to nearly 0% - as NaNO<sub>3</sub> concentration is increased from 0 g/L to 2 g/L. At the same time the leaching of REEs, B and Co remained almost constant at approximately 99%, 97% and 7%, respectively. This appreciable decrease in the level of Fe leaching can be ascribed to the oxidation of the dissolved Fe(II) ion (Eq. (7)) in the solution due to the introduction of the NaNO<sub>3</sub> oxidant.

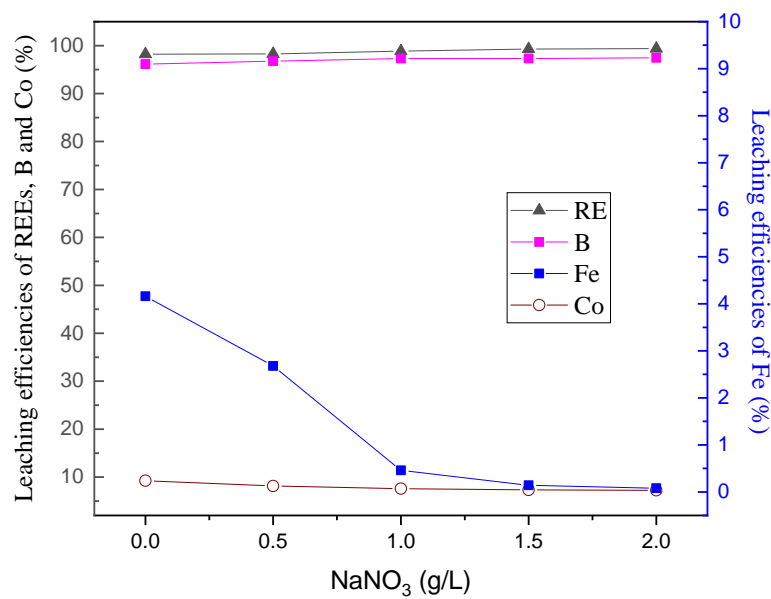
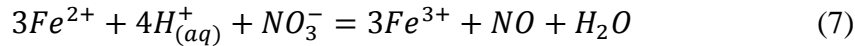


Fig. 11. Effect of NaNO<sub>3</sub> concentration on the leaching of REEs, B, Fe and Co ( $T = 180\text{ }^{\circ}\text{C}$ ;  $t = 120\text{ min}$ ;  $\text{HCl} = 0.6\text{ mol/L}$ ;  $\text{L/S} = 10$ ).

Based on the results shown in Fig. 11, the most suitable leaching conditions for the roasted spent magnet powder were determined to be HCl concentration of 0.6 mol/L, NaNO<sub>3</sub> concentration of 2 g/L, L/S ratio of 10, temperature of 180 °C and a total leaching time of 2 h. Under these conditions it was determined that > 98% REEs and < 0.1% Fe could be leached to a solution (pH 2.1), to produce the following approximate PLS composition: 19.01 g/L Nd, 4.66 g/L Pr, 1.30 g/L Dy, 0.14 g/L Gd, 0.61 g/L Ho, 0.70 g/L B with trace amounts of Fe (0.04 g/L) and Co (0.05 g/L). Additionally, the XRD results (Fig. 9) showed that the dominating phase in the leach residue was hematite (Fe<sub>2</sub>O<sub>3</sub>).

### 3.4. REEs oxalate precipitation

The effective separation of REEs and Fe can be achieved by hydrochloric acid pressure leaching as this not only helps avoid any adverse impact of impurities on product quality, but also reduces oxalic acid consumption. The effect of oxalic acid levels on the precipitation of REEs in Fe-free solution was investigated in more detail with a reaction temperature of 50 °C, initial pH = 2.2 and 30 min reaction time. As shown in Fig. 12, all of the Nd, Gd, Pr, Dy and Ho were precipitated at a  $n(\text{oxalic acid})/n(\text{REEs})$  of 1.1. When compared with high concentration iron solution (Fig. 3 and 4), the consumption of oxalic acid is significantly reduced, however when taking into account the reusability of the aqueous solution for a new leaching experiment, a value of  $n(\text{oxalic acid})/n(\text{REEs}) = 1$  was selected. At this value, 99.9% of REEs can be recovered with a REEs oxalates product purity >99.9% and almost all the oxalic acid is consumed during the precipitation process. Subsequent XRD analysis (Fig.13a) showed that the main phases with the products are hydrated REEs oxalates, with generic formula of  $\text{RE}_2(\text{C}_2\text{O}_4)_3 \cdot 4.5 \text{H}_2\text{O}$ . These oxalates have an excellent crystallinity and a particle size within the range of 1-5  $\mu\text{m}$  (Fig.13 b).

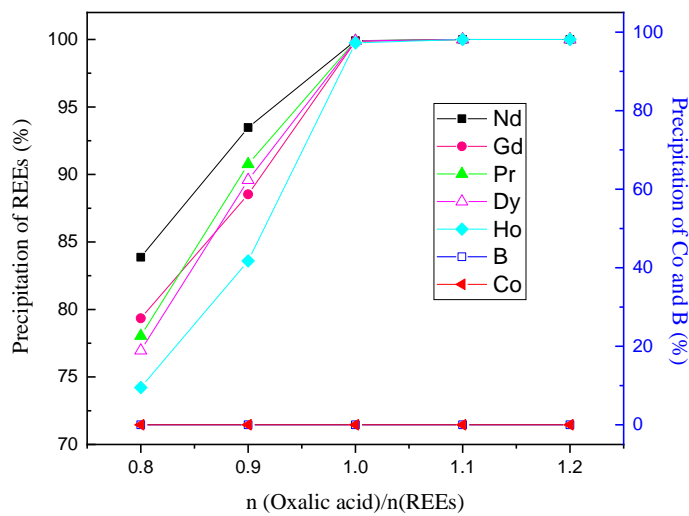
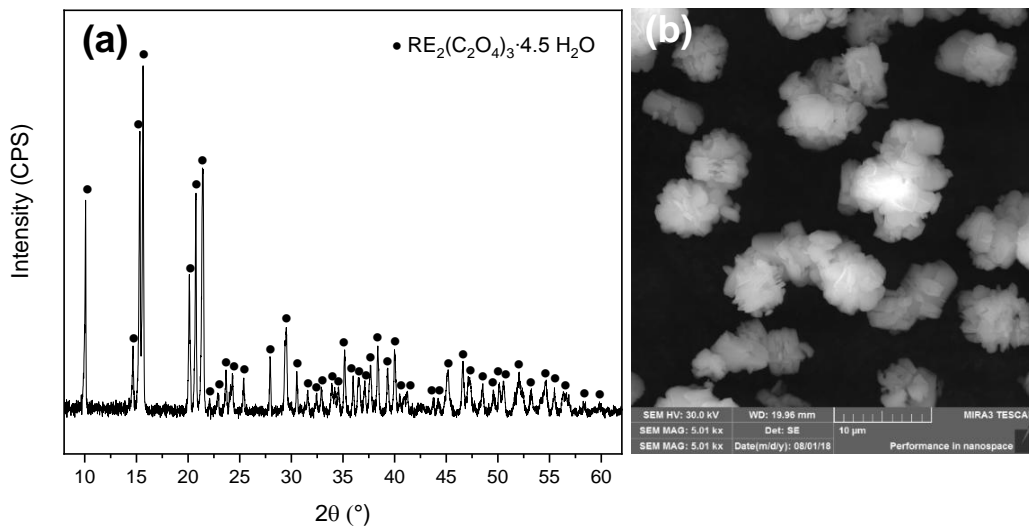


Fig. 12. Effect of the amount oxalic acid on the precipitation of REEs, Co and B



1  
2  
3  
4  
5  
6  
7  
8 Fig. 13. Characterization of REEs oxalate precipitation with (a) XRD and (b) SEM.  
9  
10

### 11 **3.5. Separation of boron from the REEs-free solution**

12 After REEs precipitation, the concentration of B and Co in the REEs-free solution were in  
13 the order of 680 mg/L and 50 mg/L (pH 0.45), with the boron mainly present as  $H_3BO_3$   
14 (Wolska and Brijak, 2013). As the B concentration is low, it is difficult to recover  
15 economically or efficiently with classical processes like co-precipitation, ion exchange and  
16 solvent extraction; therefore, it is necessary to enrich the B firstly by multiple leaching cycles.  
17 In this work, the concentration of B and Co reached levels of 3.30 g/L and 0.24 g/L after five  
18 leaching cycles. A solvent extraction method was carried out using an extractant mixture that  
19 comprised of 30% (v/v) 2-ethyl-1,3-hexanediol (EHD), 70% (v/v) sulfonated kerosene for the  
20 B recovery. Results showed that boron extraction attained was 99.5% with a three-stage  
21 counter current extraction at an O/A ratio of 1:2 at 30 °C for 10 min. A boron stripping ratio  
22 of >91.2% was achieved when the loaded organic phase was removed by NaOH (0.1mol/L)  
23 for 15 min at 30 °C with an O/A ratio of 1:2. This recovery was enhanced further by use of a  
24 three-stage counter current stripping, which resulted in B stripping ratios >99.6% and a  
25 stripping liquor containing 3.0 g/L of boron.  
26  
27  
28  
29  
30  
31  
32  
33  
34  
35  
36  
37  
38

39 After boron recovery, the  $Na_2S$  precipitation method (Vemic et al., 2016; Elwert et al.,  
40 2013) was adopted to remove the cobalt as CoS from the boron-free solution. Based on the  
41 results of the pretreatment, pressure leaching and boron solvent extraction outlined, a process  
42 flow sheet that allows for the recovery of REEs, Fe, B and Co was developed (Fig. 14).  
43 Compared with conventional methodologies, this new process has the potential to improve  
44 significantly the recovery of valuable metals, and is more environmentally friendly due to the  
45 reduced levels of boron-containing wastewater and required amounts of oxalic acid.  
46  
47  
48  
49  
50  
51  
52  
53  
54  
55  
56  
57  
58  
59  
60  
61  
62  
63  
64  
65

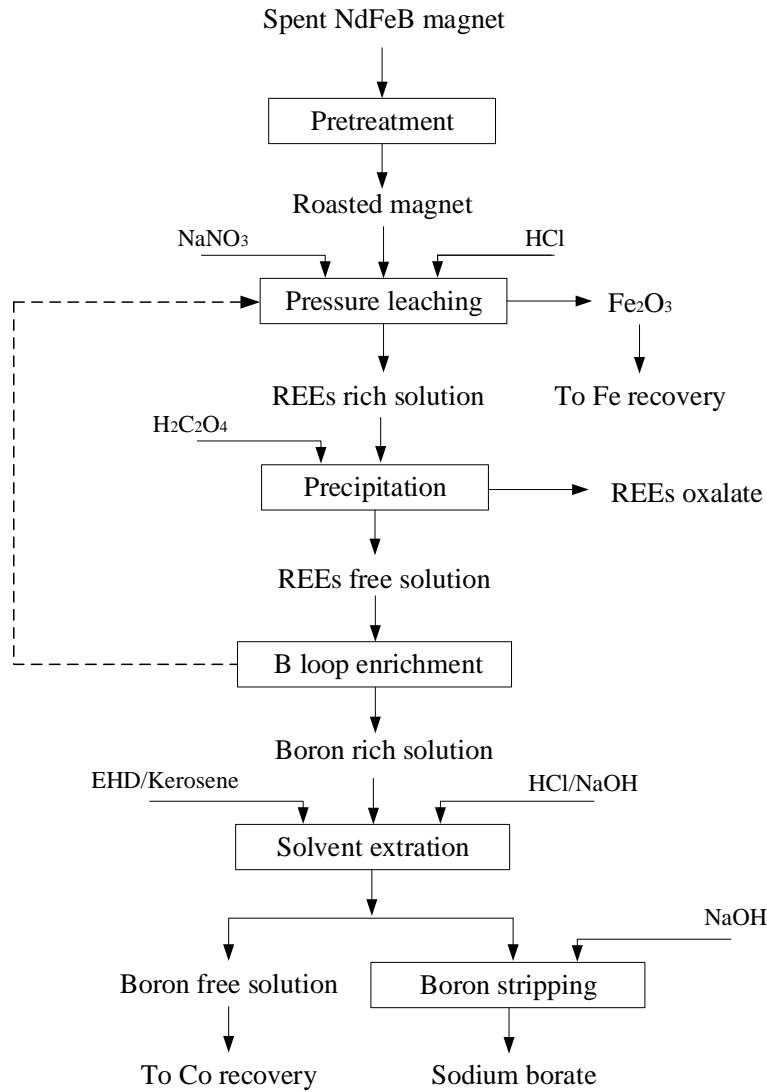


Fig. 14. Proposed flowsheet for recovery of REEs, Fe, B and Co from spent Nd-Fe-B magnets.

#### 4. Conclusions

This research outlines a novel method to separate the REEs from spent Nd-Fe-B magnets by a combined pretreatment, REEs oxalate precipitation, boron solvent extraction and cobalt precipitation process. In particular, optimization of the selective leaching of REEs vs. Fe is highlighted as this decreases both solution purification operational costs and minimizes oxalate consumption in REEs recovery stage.

For the pretreatment stage, a temperature of 800 °C was selected to avoid excessive oxidation, which leads to unsatisfactory REEs extraction, and insufficient roasting that results in poor selectivity separation of REEs and Fe. Additionally, it was found that the existence of

1 Fe(II) in the oxalate solution had a negative impact on REEs product purity, and ferric ions  
2 Fe(III) result in increased levels of oxalic acid consumption due to strong complexation  
3 between oxalate and ferric ions.-  
4

5 In the pressure-leaching step, increased temperature and prolonged leaching times can be  
6 both utilized to achieve the effective removal of Fe. Moreover, the use of NaNO<sub>3</sub> as an  
7 oxidant can radically reduce the level of Fe dissolution to <0.1%, whilst the leaching  
8 efficiencies of Nd, Pr, Dy, Gd and Ho were maintained at >98%. This clearly demonstrates  
9 that REEs and Fe can be leached selectively from roasted spent Nd-Fe-B magnet materials.  
10

11 After leaching, >99% of REEs can be precipitated by oxalic acid at the value  $n(\text{oxalic acid})/n(\text{REEs})$  of 1. Finally, 99.5% of boron is recovered by an extractant mixture composed  
12 of 30% (v/v) (EHD) and 70% (v/v) sulfonated kerosene with a three-stage counter current  
13 extraction, followed by NaOH stripping. These findings demonstrate that high recoveries of  
14 REEs, Fe and B are achievable with roasting pretreatment and hydrochloric acid pressure  
15 leaching followed oxalate precipitation and boron recovery.  
16

17 The **conventional** technical challenges such as difficulties of rare earth elements (REEs)  
18 and Fe separation, low products purity and large-scale generation of boron wastewater in the  
19 **conventional** processes have been well solved by this new developed process.  
20  
21

## 22 **Acknowledgements**

23 The authors acknowledge HYMAG project (SL/84/04.03.00.0400/2017) funded by the  
24 Regional Council of Satakunta, AIKO funding. The authors also acknowledge the financial  
25 support from the Science and Technology Project of the Education Department of Jiangxi  
26 Province (GJJ170533) as well as the National Nature Science Foundation of China  
27 (No.51804141). This paper also made use of the Academy of Finland's RawMatTERS  
28 Finland Infrastructure (RAMI) based at Aalto University.  
29  
30

## 31 **References**

32 Bandara, H.M.D., Field K.D., Emmert, M.H., 2016. Rare earth recovery from end-of-life  
33 motors employing green chemistry design principles. Green Chem. 18, 753-759.  
34

35 Battengel, A., Batnasan, A., Narankhuu, A., Haga, K., Watanabe, Y., Shibayama, A.,  
36 2018. Recovery of light and heavy rare earth elements from apatite ore using sulphuric acid  
37 leaching, solvent extraction and precipitation. Hydrometallurgy 179, 100-109.  
38  
39  
40  
41  
42  
43  
44  
45  
46  
47  
48

1 Beltrami, D., Deblonde, G.J.P., Bélair, S., Weigel, V., 2015. Recovery of yttrium and  
2 lanthanides from sulfate solutions with high concentration of iron and low rare earth content.  
3 Hydrometallurgy 157, 356–362.

4 Binnemans, K., Jones, P.T., 2015. Rare Earths and the Balance Problem. J. Sustain.  
5 Metallurgy 1 (1), 29-38.

6 Binnemans, K., Jones, P.T., 2014. Perspectives for the recovery of rare earths from end-of-  
7 life fluorescent lamps. J. Rare Earths 32, 195–200.

8 Cudennec, Y., Lecerf, A., 2006. The transformation of ferrihydrite into goethite or  
9 hematite, revisited. Journal of Solid State Chemistry 179, 716–722.

10 Du, X.Y., Graedel, T.E., 2011. Global In-Use Stocks of the Rare Earth Elements: A First  
11 Estimate. Environmental Science and Technology 45, 4096–4101.

12 Elwert, T., Goldmann, D., Schmidt, F., Stollmaier R., 2013. Hydrometallurgical recycling  
13 of sintered NdFeB magnets. World Metall 66(4), 209-219.

14 Firdaus, M., Rhamdhani, M.A., Rankin, W.J., Pownceby, M., Webster, N. A. S.,  
15 D'Angelo, A.M., Kathie McGregor, K., 2018. High temperature oxidation of rare earth  
16 permanent magnets. Part 1-Microstructure evolution and general mechanism. Corrosion  
17 Science 133, 374-385.

18 Hoogerstraete, V., Blanpain, B., Gerven, T.V., Binnemans, K., 2014. From NdFeB  
19 magnets towards the rare-earth oxides: a recycling process consuming only oxalic acid. RSC  
20 Adv. 4, 64099-64111.

21 Horikawa, T., Miura, K., Itoh, M., Machida, K.I., 2006. Effective recycling for Nd–Fe–B  
22 sintered magnet scraps. Journal of Alloys and Compounds 408-412, 1386-1390.

23 Hubli, R.C., Mitra, J., Suri, A.K., 1997. Reduction-dissolution of cobalt oxide in acid  
24 media: a kinetic study, Hydrometallurgy 44, 25-114.

25 Itoh, M., Miura, K., Machida, K., 2008. Novel rare earth recovery process on Nd–Fe–B  
26 magnet scrap by selective chlorination using NH<sub>4</sub>Cl. J Alloys Comp 477, 484-487.

27 Jha, M.K., Kumari A., Panda R., Kumar, J.R., Yoo, K., Lee, J.Y., 2016. Review on  
28 hydrometallurgical recovery of rare earth metals. Hydrometallurgy 161, 77-101.

29 Koyama, K., Kitajima, A., Tanaka, M., 2009. Selective leaching of rare-earth elements  
30 from an Nd-Fe-B magnet. Kidorui (Rare Earths) 54, 36-37.

31 Kruse, S., Raulf, K., Pretz, T., Friedrich, B., 2017. Influencing factors on the melting  
32 characteristics of NdFeB-Based production wastes for the recovery of rare earth compounds.  
33 Journal of Sustainable Metallurgy 3, 168-178.

34 Kumari, A., Sinha, M. K., Pramanik, S., Sahu, S. K., 2018. Recovery of rare earths from  
35 spent NdFeB magnets of wind turbine: Leaching and kinetic aspects. Waste Management 75,  
36 486-498.

37 Langová, Š., Matýsek, D., 2010. Zinc recovery from steel-making wastes by acid pressure  
38 leaching and hematite precipitation. Hydrometallurgy 101, 171-173.

39 Lee, C.H., Chen, Y.J., Liao, C.H., Popuri, S.R., Tsai, S.L., Hung, C.E., 2013. Selective  
40 leaching process for neodymium recovery from scrap Nd-Fe-B magnet. Metall. Mater. Trans.  
41 A 44, 5825-5833.

42  
43  
44  
45  
46  
47  
48  
49  
50  
51  
52  
53  
54  
55  
56  
57  
58  
59  
60  
61  
62  
63  
64  
65

1 Lee, J.C., Kim, W.B., Jeong, J., Yoon, I.J., 1998. Extraction of neodymium from Nd-Fe-B  
2 magnet scraps by sulfuric acid. *J Korean Inst Met Mater* 36(6), 967-972.

3 Liu, F.P., Liu, Z.H., Li, Y.H., Wilson, B.P., Lundström, M., 2017. Extraction of Ga and  
4 Ge from zinc refinery residues in H<sub>2</sub>C<sub>2</sub>O<sub>4</sub> solutions containing H<sub>2</sub>O<sub>2</sub>. *International Journal of*  
5 *Mineral Processing* 163, 14 - 23.

6  
7 Lyman, J.W., Palmer, G.R., 1993. Recycling of rare earths and iron from NdFeB magnet  
8 scrap. *High Temp. Mater. Proc.* 11, 175–187.

9  
10 Morgan, B., Lahav, O., 2007. The effect of pH on the kinetics of spontaneous Fe(II)  
11 oxidation by O<sub>2</sub> in aqueous solution--basic principles and a simple heuristic description.  
12 *Chemosphere* 68 (11), 2080-2084.

13  
14 Murase, K., Machida, K., Adachi, G., 1995. Recovery of rare metals from scrap of rare  
15 earth inter-metallic material by chemical vapor transport. *J Alloys Comp* 217, 218-225.

16  
17 Önal, M.A.R., Borra, C.R., Guo, M.X., Blanpain, B., Gerven, T.V., 2015. Recycling of  
18 NdFeB Magnets Using Sulfation, Selective Roasting, and Water Leaching. *J. Sustain. Metall.*  
19 *1*, 199-215.

20  
21 Önal, M.A.R., Borra, C.R., Guo, M.X., Blanpain, B., Gerven, T.V., 2017.  
22 Hydrometallurgical recycling of NdFeB magnets: Complete leaching, iron removal and  
23 electrolysis. *Journal of rare earths* 35(5), 574-583.

24  
25 Önal, M.A.R., Aktan, E., Borra, C.R., Blanpain, B., Gerven, T.V., Guo, M.X., 2017.  
26 Recycling of NdFeB magnets using nitration, calcination and water leaching for REE  
27 recovery. *Hydrometallurgy* 167, 115-123.

28  
29 Panayotova, M., Panayotov, V., 2012. Review of methods for the rare earth metals  
30 recycling. *Annual of the University of Mining and Geology, St. Ivan Rilski, Min. Miner.*  
31 *Process.* 55, 142-147.

32  
33 Petranikova, M., Herdzik-Koniecko, I., Steenari, B.M., Ekberg, C., 2017.  
34 Hydrometallurgical processes for recovery of valuable and critical metals from spent car  
35 NiMH batteries optimized in a pilot plant scale. *Hydrometallurgy* 171, 128-141.

36  
37 Rabatho, J. P., Tongamp, W., Takasaki, Y., Haga, K., Shibayama, A., 2013. Recovery of  
38 Nd and Dy from rare earth magnetic waste sludge by hydrometallurgical process. *J Mater*  
39 *Cycles Waste Manag* 15, 171-178.

40  
41 Radwan, N.R.E., EI-Shobaky, 2000. Solid–solid interactions between ferric and cobalt  
42 oxides as influenced by Al<sub>2</sub>O<sub>3</sub>-doping. *Thermochimica Acta* 360(2), 147-156.

43  
44 Riveros, P.A., Dutrizac, J.E., 1997. The precipitation of hematite from ferric chloride  
45 media. *Hydrometallurgy* 46, 85-104.

46  
47 Saito, T., Sato, H., Ozawa, S., Yu J., Motegi T., 2003. The extraction of Nd from waste  
48 Nd–Fe–B alloys by the glass slag method. *J Alloys Comp* 353, 189 -193.

49  
50 Sasaki, K., Qiu, X., Hosomomi, Y., Moriyama, S., Hirajima, T., 2013. Effect of natural  
51 dolomite calcination temperature on sorption of borate onto calcined products. *Microporous*  
52 *Mesoporous Mater.* 171, 1-8.

53  
54 Sun, M., Hu, X., Peng, L., Fu, P., Ding, W., Peng, Y., 2015. On the production of Mg-Nd  
55 master alloy from NdFeB magnet scraps. *J. Mater. Proc.* 218, 57-61.

56  
57  
58  
59  
60  
61  
62  
63  
64  
65

1 Tagliabue, M., Reverberi, A.P., Bagatin, R., 2014. Boron removal from water: needs,  
2 challenges and perspectives. *Journal of Cleaner Production* 77, 56-64.

3 Tang, C.W., Wang, C.B., Chien, S.H., 2008. Characterization of cobalt oxides studied by  
4 FT-IR, Raman, TPR and TG-MS. *Thermochimica Acta* 473(1-2), 68-73.

5 Tu, K.L., Nghiem, L.D., Chivas, A.R., 2010. Boron removal by reverse osmosis  
6 membranes in seawater desalination applications. *Sep. Purif. Technol.* 75, 87-101.

7  
8 Tunsu, 2018. Hydrometallurgy in the recycling of spent NdFeB permanent magnets,  
9 *Waste Electrical and Electronic Equipment Recycling* 8, 175-211.

10  
11 Vemic, M., Bordas, F., Comte, S., Guibaud, G., Lens P.N.L., Hullebusch, E.D.V., 2016.  
12 Recovery of molybdenum, nickel and cobalt by precipitation from the acidic leachate of a  
13 mineral sludge. *Environmental Technology* 37 (17), 2231-2242,  
14  
15

16 Venkatesan, P., Sun, Z., Sietsma, J., Yang, Y.Y., 2018. An environmentally friendly  
17 electro-oxidative approach to recover valuable elements from NdFeB magnet waste.  
18 *Separation and Purification Technology* 191, 384-391.  
19

20 Wolska, J., Brijak, M., 2013. Methods for boron removal from aqueous solutions. A  
21 review. *Desalination* 310, 18-24  
22

23 Xu, Y., Jiang, J.Q., 2008. Technologies for boron removal. *Ind. Eng. Chem. Res.* 47, 16-  
24 24.  
25

26 Yang, Y.X., Walton, A., Sheridan, A., Guth, K., Gauß, R., Gutfleisch, O., Buchert, M.,  
27 Steenari, B.M., Gerven, T.V., Jones, P.T., Binnemans, K., 2017. REE Recovery from End-of-  
28 Life NdFeB Permanent Magnet Scrap: A Critical Review, *J. Sustain. Metall.* 3, 122-149.  
29  
30

31 Yoon, H.S., Kim, C.J., Chung, K.W., Jeon S., Park I, Yoo, K., Jha, M.K., 2015. The Effect  
32 of Grinding and Roasting Conditions on the Selective Leaching of Nd and Dy from NdFeB  
33 Magnet Scraps, *Metals* 5, 1306-1314.  
34

35 Zhou, X., Tian, Y.L., Yu, H.Y., Zhang, H., Zhong, X.C., Liu, Z.W., 2019. Synthesis of  
36 hard magnetic NdFeB composite particles by recycling the waste using microwave assisted  
37 auto-combustion and reduction method. *Waste Management* 87, 645–651.  
38  
39  
40  
41  
42  
43  
44  
45  
46  
47  
48  
49  
50  
51  
52  
53  
54  
55  
56  
57  
58  
59  
60  
61  
62  
63  
64  
65

# Recovery and separation of rare earths and boron from spent Nd-Fe-B magnet

Fupeng Liu<sup>1,2</sup>, Antti Porvali<sup>2</sup>, JinLiang Wang<sup>1</sup>, Houqing Wang<sup>1</sup>, Chao Peng<sup>2</sup>, Benjamin P. Wilson<sup>2</sup>, Mari Lundström<sup>2</sup>

<sup>1</sup> Institute of Engineering Research, Jiangxi University of Science and Technology, Ganzhou, 341000, China.

<sup>2</sup> Hydrometallurgy and Corrosion, Department of Chemical and Metallurgical Engineering (CMET), School of Chemical Engineering, Aalto University, P.O. Box 12200, FI-00076 AALTO, Finland.

## Abstract:

The environmental and economic benefits of recycling spent Nd-Fe-B magnets are becoming increasingly important. Nevertheless, the reprocessing of this type of material by existing processes remains a challenge due to the difficulties of rare earth elements (REEs) and Fe separation, low products purity and large-scale generation of boron wastewater. This research presents an effective approach for the comprehensive recovery of REEs, iron and boron from spent Nd-Fe-B magnet wastes. Investigations of the initial roasting pretreatment showed it to be an effective method that aids the subsequent selective separation of REEs, with the most suitable temperature determined to be 800 °C. During the following selective hydrochloric acid pressure leaching of the roasted magnet, the addition of 2 g/L NaNO<sub>3</sub> was found to significantly improve the separation of REEs and B from Fe. The results indicated that almost 99% of REEs and 97% of B could be extracted, whilst in contrast, less than 0.1% of iron dissolved, to leave a hematite rich residue. The extracted REEs were then directly precipitated as oxalates with > 99% extraction and 99.95% purity at a value  $n(\text{oxalic acid})/n(\text{REEs})$  of 1, resulting in significant improvements to oxalic acid consumption and REEs product purity. In the final step, 99.5% of boron was recovered via a three-stage counter current extraction with 30% (v/v) (EHD) and 70% (v/v) sulfonated kerosene. These findings demonstrate that high recoveries of REEs, Fe and B are achievable with hydrochloric acid pressure leaching followed oxalate precipitation and boron recovery.

**Keywords:** Spent Nd-Fe-B magnet; Pressure leaching; Rare earth; Boron; Hematite

## 1. Introduction

Rare earth elements (REEs) are important strategic resources due to their unique properties and have been extensively used in a variety of high-technology fields, such as high-temperature superconductors, NiMH batteries, fluorescent lamps, permanent magnets

1 and catalysts (Jha et al., 2016; Petranikova et al., 2017; Hoogerstraete et al., 2014; Binnemans  
2 and Jones, 2014; Panayotova and Panayotov, 2012). Annually, almost 22% (approx. 26 000  
3 tons) of all REEs produced worldwide are utilized in the production of Nd-Fe-B magnets.  
4 Such magnets form the largest application among REEs (Nd, Pr, Gd, Dy and Ho) - both in  
5 terms of tonnage and market value - and it has been estimated that total Nd-Fe-B magnet  
6 production will reach 120,000 tons by 2020 (Yang et al. 2017; Benecki et al., 2011). The  
7 maximum lifetime of a Nd-Fe-B permanent magnet depends on its application and can range  
8 from just 2 - 3 years in the case of consumer electronics to 20 - 30 years for wind turbines  
9 (Du and Graedel, 2011; Yang et al., 2017; Tunsu, 2018). This has led to significant and  
10 increasing quantities of Nd-Fe-B magnet waste being generated both as a result of production  
11 – approx. 20 - 30% of the alloy is turned to scrap during processing – and disposal of  
12 permanent magnets at the end of their useful service life (Horikawa et al., 2006; Kumari et al.,  
13 2018). Recycling of the spent magnets is attractive since the material comprises of 30 - 40%  
14 REEs (Önal et al., 2017), however, global commercial recycling rates of end-of-life REEs  
15 products is currently estimated to be < 1% (Binnemans et al., 2015; Tunsu, 2018).  
16 Consequently, there is a need to develop new processes for the effective recycling of these  
17 spent magnets that not only provide environmental benefits but also are economically viable  
18 on an industrial scale.

19  
20  
21  
22  
23  
24  
25  
26  
27  
28  
29  
30  
31  
32  
33 In addition to the REEs, the other predominant metal in spent magnets is iron that  
34 comprises *ca.* 50 - 70% of the total mass and as a result, any recovery methodology must be  
35 able to separate effectively REEs from Fe (Venkatesan et al., 2018). Although some  
36 pyrometallurgical processes like liquid metal extraction (Sun et al., 2015), selective  
37 chlorination (Itoh et al., 2008), glass slag method (Saito et al., 2003), chemical vapor  
38 transport (Murase et al., 1995) and sulfate or nitrate selective roasting (Önal et al., 2015; Önal  
39 et al., 2017) have been developed to separate REEs and Fe, some of these pyrometallurgical  
40 methods are highly energy intensive, low recovery efficiencies of REEs and may also result  
41 in secondary environmental pollution. In contrast, hydrometallurgical approaches can offer an  
42 alternative that allows high purity REEs products to be obtained with lower levels of  
43 associated air pollution (Kumari et al., 2018; Jha et al., 2018). For example, in the early  
44 1990s, Lyman and Palmer (1993) developed a method that utilizes sulfuric acid leaching  
45 followed by sulfate double salt precipitation, which results in almost 98% of REEs being  
46 extracted with 2 mol/L H<sub>2</sub>SO<sub>4</sub> and L/S ratio of 10 at ambient temperature. Nevertheless, REE  
47 solution enrichment to high concentrations is not possible due to the low solubility of REE  
48 sulfates, whereas some heavy REEs like Dy and Ho are lost due to their incomplete  
49  
50  
51  
52  
53  
54  
55  
56  
57  
58  
59  
60  
61  
62  
63  
64  
65

1 precipitation by the double sulfate precipitation process (Beltrami et al., 2015; Battsengel et  
2 al., 2018).

3  
4 Several efforts have been made to eliminate the negative influence of sulfate ion by the use  
5 of alternative leaching systems based on nitric, hydrochloric and acetic acids. The results  
6 showed that high levels (>95%) of both REEs and Fe were leached due to the higher  
7 solubility of REEs in chloride and nitrate media (Lee et al., 2013; Önal et al., 2017). The  
8 main drawbacks to these methods is that the presence of large amounts of dissolved iron not  
9 only hinders REEs oxalate precipitation, - a typical industrial process for REEs separation -  
10 but also makes the subsequent purification more complex, resulting in increased costs and  
11 low-value products such as Fe(OH)<sub>3</sub>, and Fe/Co containing REEs oxalates (Bandara et al.,  
12 2016; Venkatesan et al., 2018). As a result, alternative methods of selective leaching  
13 processes have been developed to overcome the disadvantages of complete leaching. Rabatho  
14 et al. (2013) studied a leaching system composed of a 1mol/L HNO<sub>3</sub> and 0.3 mol/L H<sub>2</sub>O<sub>2</sub>  
15 mixture, which could dissolve 70 -90% of REEs and < 15% of Fe from spent magnet in 5 min  
16 at 80 °C. Nonetheless, 20 - 30% losses of Nd and Dy were observed during the iron removal  
17 step, whereas the use of HNO<sub>3</sub> and H<sub>2</sub>O<sub>2</sub> significantly increases the operational cost.

18  
19 Another alternative method that has been widely adopted for REEs recovery is the  
20 oxidative roasting – selective leaching process (Koyama et al., 2009; Lee et al., 1998;  
21 Hoogerstraete et al., 2014; Kumari et al., 2018). In this process, accurate control the roasting  
22 is essential as insufficient oxidation of the Nd<sub>2</sub>Fe<sub>14</sub>B causes some of iron to dissolve into the  
23 solution as ferrous ion, the pH stability of which subsequently inhibits the selective leaching  
24 of REEs. On the other hand, excessive roasting leads to the formation of partial insoluble  
25 ferrites like NdFeO<sub>3</sub> that also make high recovery efficiencies of REEs a challenge (Lee et  
26 al., 1998; Önal et al., 2015; Firdaus et al., 2018).

27  
28 After roasting, Hoogerstraete et al. (2014) investigated low concentration hydrochloric  
29 acid leaching for roasted magnet waste and found that almost all the iron remains in the leach  
30 residue if the molar ratio of HCl and REEs is optimized. However, the complete separation of  
31 REEs and iron could only be achieved after 15 h with a  $n(\text{HCl})/n(\text{REEs})$  ratio of 3.5 at 80 °C,  
32 and the dissolved iron in the leachate was mainly precipitated as Fe(OH)<sub>3</sub> or FeOOH (at pH >  
33 1.5). Kumari et al. (2018) found that the leaching kinetics are controlled by both diffusion  
34 through the solution boundary layer and the chemical reaction at the interface, therefore both  
35 longer reaction duration and increased temperature can enhance REEs leaching. In addition,  
36 Koyama et al. (2009) found that more than 99% of the REEs content of Nd-Fe-B spent  
37  
38  
39  
40  
41  
42  
43  
44  
45  
46  
47  
48  
49  
50  
51  
52  
53  
54  
55  
56  
57  
58  
59  
60  
61  
62  
63  
64  
65

1 magnets could be dissolved in 0.02 mol/L HCl with an industrially irrelevant low L/S (mL/g)  
2 ratio of 1000 ( $T = 180\text{ }^{\circ}\text{C}$ ,  $t = 2\text{h}$ ) with  $< 0.5\%$  of related Fe dissolution.

3  
4 The advantage of pressure leaching is that the iron mainly exists in the leaching residue as  
5 hematite ( $\text{Fe}_2\text{O}_3$ ), which - when compared to ferrihydrite  $\text{Fe}(\text{OH})_3$ , akaganeite ( $\text{FeOOH}$ ) and  
6 jarosite ( $\text{MFe}_3(\text{SO}_4)_2(\text{OH})_6$ ) - has some significant advantages like good environmental  
7 stability, low cation adsorption capacity and potential marketability to the steel industry  
8 ([Riveros and Dutrizac, 1997](#)). The drawback of the method outlined by [Koyama et al. \(2009\)](#)  
9 is that a high liquid-solid ratio makes the subsequent enrichment and recovery of REEs from  
10 very dilute solutions problematic. In addition, as the application range of the process is  
11 narrow, it is difficult to achieve selective separation of iron for materials that are not fully  
12 oxidized due to the sluggish oxidation kinetics of Fe(II) in the acidic leachate ( $\text{pH} < 4$ )  
13 ([Morgan and Lahav, 2007](#)). Although the introduction of  $\text{H}_2\text{O}_2$  can obviously promote the  
14 iron removal in the pressure leaching ([Langová and Matýšek, 2010](#)), the consumption of  
15  $\text{H}_2\text{O}_2$  is large because of the thermolabile nature of  $\text{H}_2\text{O}_2$  ([Liu et al., 2017](#)).

16  
17 Another challenge in the recycling of spent Nd-Fe-B magnets is the removal of boron.  
18 Currently, most research focuses on the recovery of valuable metals such as REEs, Co and Fe,  
19 although there are a few reports on boron retrieval from spent magnet waste ([Tunsu, 2018](#);  
20 [Jha et al., 2018](#)). Nevertheless, the ability to reclaim also boron is necessary in order to avoid  
21 its accumulation into products or wastewaters during the recycling process. Additionally, the  
22 recovery of boron can allow its circulation either back to the industrial manufacture of  
23 permanent magnets or other uses like the production of fiberglass, detergents, fertilizers, etc.  
24 ([Tagliabue et al., 2014](#); [Wolska and Brijak, 2013](#)). Although adsorption separation and  
25 membrane filtration processes have been widely applied to boron recovery from low  
26 concentration boron solutions such as desalinate seawater and salt lake brine ([Sasaki et al.,](#)  
27 [2013](#); [Tu et al., 2010](#); [Xu et al., 2008](#)), these methods are not suitable for acidic solutions  
28 containing high concentrations of B.

29  
30 In the current study, a new pressure leaching approach for Nd-Fe-B magnets is taken by  
31 introducing  $\text{NaNO}_3$  as the assistant reagent. By this method, the separation between REEs  
32 and Fe leaching could be significantly improved. In order to present a complete process  
33 scheme for spent Nd-Fe-B magnets, the current work investigates not only the selective  
34 pressure acid leaching process, but also the subsequent REEs oxalates recovery and boron  
35 removal by a 2-ethyl-1,3-hexanediol/sulfonated kerosene solvent combination, with the focus  
36 on behavior of impurities and valuable metals during each process step.  
37  
38  
39  
40  
41  
42  
43  
44  
45  
46  
47  
48  
49  
50  
51  
52  
53  
54  
55  
56  
57  
58  
59  
60  
61  
62  
63  
64  
65

## 2. Experimental

### 2.1. Experimental procedure

#### 2.1.1. Pretreatment and pressure leaching

Spent Nd-Fe-B magnets, obtained from a company in Finland, were firstly demagnetized in a muffle furnace (air atmosphere) by heating at 350 °C for 1h, before being crushed and ground in a mill (Pulverisette 9, Fritsch, Germany). It need to be noted that as the particle size of magnet waste decreases the waste will become pyrophoric in character, readily reacting with the heat of the milling and oxygen present in the air (Kruse et al., 2017). Once ground, the sample was further roasted in the air at different temperatures (700 °C; 800 °C; 900 °C) for 2h. The pressure acid leaching test was performed by mixing the roasted spent magnet and hydrochloric acid solution at a pre-determined L/S ratio in a 1 L titanium autoclave with agitator speed 300 r/min. The temperature and pressure range were listed in the Table 1. After filtration, the leach residue was washed with deionized water and both the residue and filtrate samples were analyzed. The leaching efficiency (%E) is defined as:

$$\%E = (C_M \times V)/(m \times w_M) \times 100\% \quad (1)$$

Where  $C_M$  is the concentration of metals in the leachate (g/L);  $V$  is the volume of leachate (L);  $m$  is the mass of input spent NdFeB magnet (g) and  $w_M$  is the amount of an element in the roasted magnet.

#### 2.1.2. REEs oxalate precipitation

In order to investigate the REEs oxalates precipitation phenomena, the effect of ferrous and ferric ion on the recovery and purity of REEs oxalate was investigated by a synthetic solution with  $[Nd^{3+}] = 20$  g/L and different concentrations of ferrous ions and ferric ions. Then, the oxalic acid was directly added into the simulated solution with  $n(\text{oxalic acid})/n(\text{REEs})$  of 1.5 ( $t = 1\text{h}$ ,  $T = 50$  °C). In addition, the consumption of oxalic acid in high concentration iron (10 g/L) solution and Fe-free solution was investigated under the same experimental conditions. Afterwards, the resultant precipitate was filtered, washed with distilled water before being dried at 100 °C. The precipitation of REEs (%P) was calculated as follows:

$$\%P = (1 - C_1/C_0) \times 100\% \quad (2)$$

Where  $C_0$  and  $C_1$  represent the initial and final concentration of REEs before and after precipitation procedure, respectively.

### 2.1.3. Boron solvent extraction

After the REEs precipitation, dissolved boron was extracted and enriched by solvent extraction. The extraction experiments were carried out in 125 mL separation funnels by mixing an organic phase and the aqueous solution, with different organic/aqueous phase (O/A) ratios, at 30 °C for 10 min in an incubator shaker (Model KS 3000i, IKA, Germany) . The organic phase consisted of 30% (v/v) 2-ethyl-1,3-hexanediol and 70% (v/v) sulfonated kerosene (both provided by Shanghai Rare-earth Chemical Co., Ltd., China) as the solvent for extraction. The loaded organic phase was subsequently stripped with 0.1 mol/L NaOH for 15 min at an O/A ratio of 1:2 and 30 °C.

The investigated parameters utilized at each processing stage are displayed in Table 1. All chemical reagents utilized were of analytical grade and deionized water was used throughout the experiments for the solution preparation.

Table 1. Main parameters investigated during the experiments.

Experiments	Investigated Parameters
Oxidative Roasting	Temperature: 600-900 °C; Roasting time: 120 min;
Pressure Leaching	Liquid-to-solid (L/S): 4-12 ml/g; Temperature: 100-200 °C; HCl: 0.2-0.8 mol/L; Reaction time: 20-180 min; NaNO <sub>3</sub> : 0-2 mg/L
Oxalate Precipitation	Temperature: 25-50 °C; $n(\text{oxalic acid})/n(\text{REEs})$ : 0.8-1.2; Reaction time: 10-180 min; Fe <sup>3+</sup> : 0-15 g/L
Boron Solvent Extraction	Reaction time: 5–15 min; temperature: 30 °C; N235(v/v): 5–10%; organic/aqueous phase ratio (v/v) (O:A): 2:1–1:6

## 2.2. Analytical methods

The chemical analysis of the spent magnet, leaching residues and products formed were performed using a number of different spectroscopic techniques. Firstly, the solid samples were subjected to total dissolution in aqua regia, then the resultant solution concentrations of REEs, Fe, Co, B and other impurities were determined by inductively coupled plasma-optical

1 emission spectroscopy (ICP-OES, Perkin Elmer Optima 7100 DV, USA). The Fe(II)  
2 concentrations in the spent magnet and leaching residues were analyzed by the chemical  
3 dissolution - potassium dichromate method. In contrast, the Fe(III) concentrations in leachate  
4 were analyzed by a precipitation separation - EDTA titration method (Liu et al, 2017). EPMA  
5 - Electron-Probe X-ray Microanalysis, of the Fe and REEs (Nd, Pr, Gd, Dy and Ho)  
6 distribution behaviors were measured by a JEOL JXA-8230 instrument operated at 15 kV  
7 with a 10 nA beam current. The main mineral phases within the samples were identified by  
8 XRD (PANalytical X'Pert Pro Powder, Almelo, the Netherlands) using a CoK $\alpha$  radiation  
9 source with a 40 kV acceleration potential and current of 40 mA. XRD diffractograms were  
10 analyzed by using HighScore 4.0 Plus software. The morphology and size of the REEs  
11 products were determined by SEM (A LEO 1450, Carl Zeiss Microscopy GmbH, Jena,  
12 Germany). All the other chemicals used in the leaching, precipitation and solvent extraction  
13 were of analytical grade.  
14  
15  
16  
17  
18  
19  
20  
21  
22  
23  
24

### 25 **3. Results and discussion**

#### 26 **3.1. Spent NdFeB magnet pretreatment**

27 After demagnetization, crushing and grinding, ca. 80% of the particles in the spent magnet  
28 powder were < 160  $\mu$ m. Fig. 1 shows the EPMA results for distributions of Fe, Dy, Gd, Ho,  
29 Nd and Pr in the material. The results indicate that most of rare earth elements mainly co-  
30 exist with Fe, but also that some REEs like Nd, Gd and Pr have their own independent phase.  
31 These independent phases are akin to inclusions within the Fe matrix, which necessitate very  
32 fine grinding to ensure the best recovery of the REEs.  
33  
34  
35  
36  
37  
38  
39

40 After grinding, oxidation roasting with different temperatures (700°C, 800°C and 900°C)  
41 was undertaken, and the roasting time was 2 h. XRD results, shown in Fig. 2, indicate that the  
42 roasting temperature of 700 °C led to the incomplete oxidation of both the Fe and REEs in  
43 the spent magnet as Nd<sub>2</sub>Fe<sub>14</sub>B diffraction peaks are still present. The presence of unoxidized  
44 Fe leads to problems in the subsequent process steps as it will dissolve during leaching and  
45 remain in the solution as Fe<sup>2+</sup> up to pH value of 6-8. In contrast at  $T = 900$  °C, NdFeO<sub>3</sub> is  
46 clearly formed, which significantly suppresses the leaching of REEs. Consequently, a too  
47 high oxidation temperature will result in poor REEs extraction, whereas insufficient roasting  
48 will cause poor selectivity due to Fe<sup>2+</sup> dissolution. Based on the roasting results, 800 °C was  
49 selected as the most suitable roasting temperature. The contents of REEs, Fe and other main  
50 elements of interest found in the spent magnet powder before and after roasting at 800 °C are  
51  
52  
53  
54  
55  
56  
57  
58  
59  
60  
61  
62  
63  
64  
65

shown in Table 1. As it can be seen, the content of Fe decreased from 62.7 to 46.4% before and after roasting, which indicates a net mass gain by 35.1% for the sample. REEs including Nd, Pr, Dy, Gd and Ho accounted for 25.8% of the total elements, whereas the B and Co content were both > 0.6%.

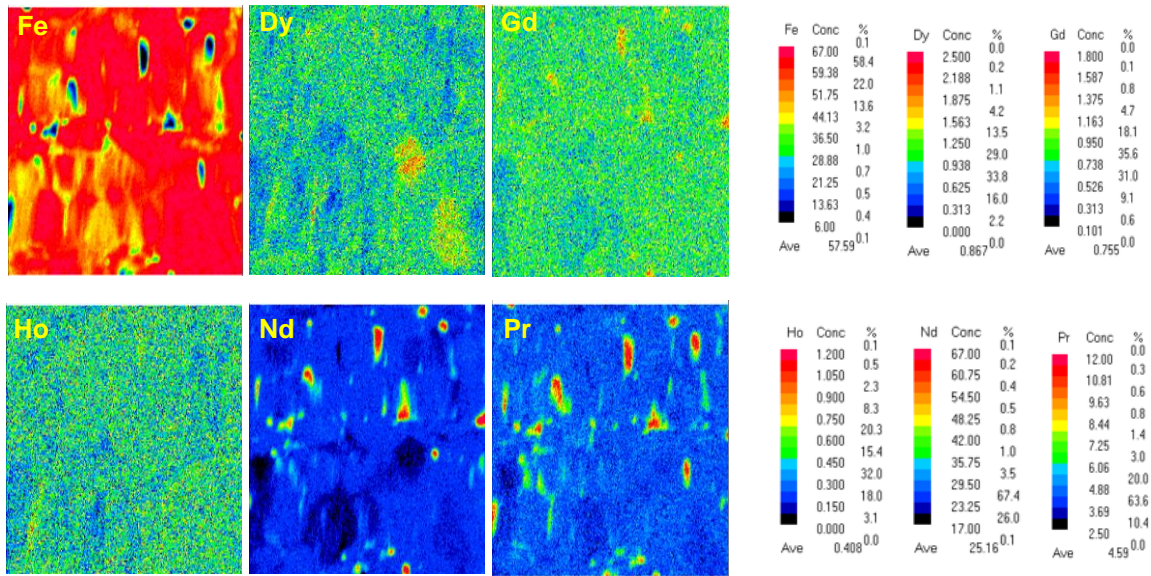


Fig. 1. EPMA distribution maps of Fe, Pr, Nd, Dy, Gd and Ho in the spent magnet powder.

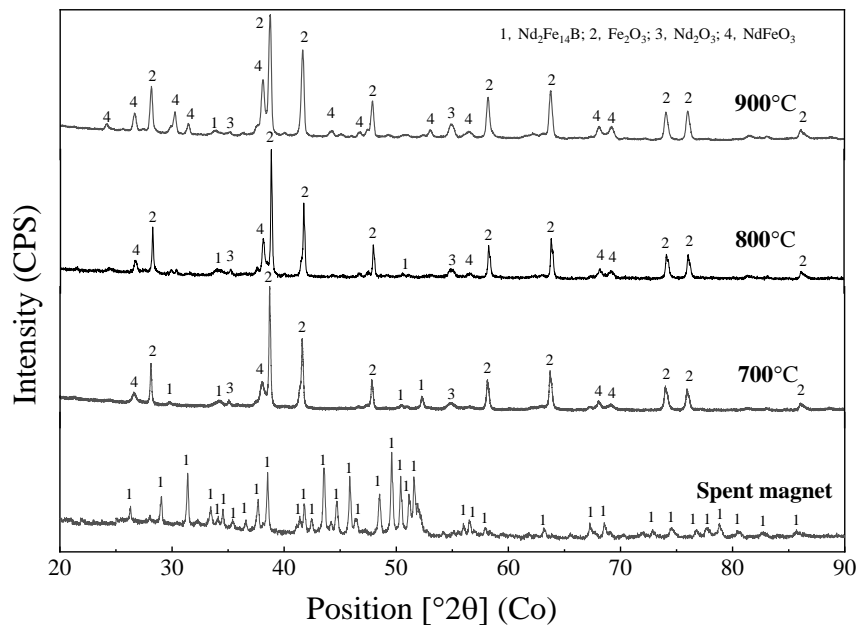


Fig. 2. XRD pattern of the spent Nd-Fe-B magnet powder before and after roasting.

Table 1. Chemical composition of spent Nd-Fe-B magnet powder before and after roasting

Elements	Fe	Nd	Pr	Dy	Gd	Ho	B	Co
Before (wt. %)	62.67	25.81	6.10	1.80	0.19	0.84	0.96	0.87
After (wt. %)	46.38	19.19	4.55	1.33	0.14	0.62	0.71	0.64

### 3.2. REEs oxalate precipitation in high concentration iron solution

From the analysis of the raw materials, it was found that the iron content was as high as 50%, which in the traditional hydrochloric acid leaching or sulfuric acid leaching of magnet waste makes the leaching of Fe inevitable. In order to determine the effect of Fe on the REEs oxalate precipitation behavior, the REEs oxalic acid precipitation was investigated in synthetic solution at different concentrations of the ferrous and ferric ion. The purity of the precipitate was found to increase from 98.5% to 99.9% as the proportion of ferric ion increases from zero to 100% (Fig. 3). However, the associated precipitation efficiencies of the REEs decreased significantly from 98.6% to 76.0%. It is clear that the presence of Fe(II) in the oxalate solution had a negative impact on the purity of REEs products and that ferric ions result in a substantial increase in oxalic acid consumption, due to the strong complexation of oxalate anion with ferric cation (Liu et al., 2017).

Fig. 4 shows that the REEs precipitation is above 99.0% when the value of  $n(\text{oxalic acid})/n(\text{REEs})$  reaches 3.0. This means that there are still notable amounts of dissolved oxalic acid present that results in oxalate accumulation within the aqueous phase. Evidently, a low concentration of Fe in solution is beneficial for the process, as it enhances REEs recovery and minimizes the oxalate accumulation in the pregnant leach solution (PLS). In the current work, a strategy of minimal Fe dissolution was achieved by adopting a high pressure leaching process for the roasted spent magnet material, which allows to convert the dissolved iron into hematite prior to the REE oxalate precipitation stage.

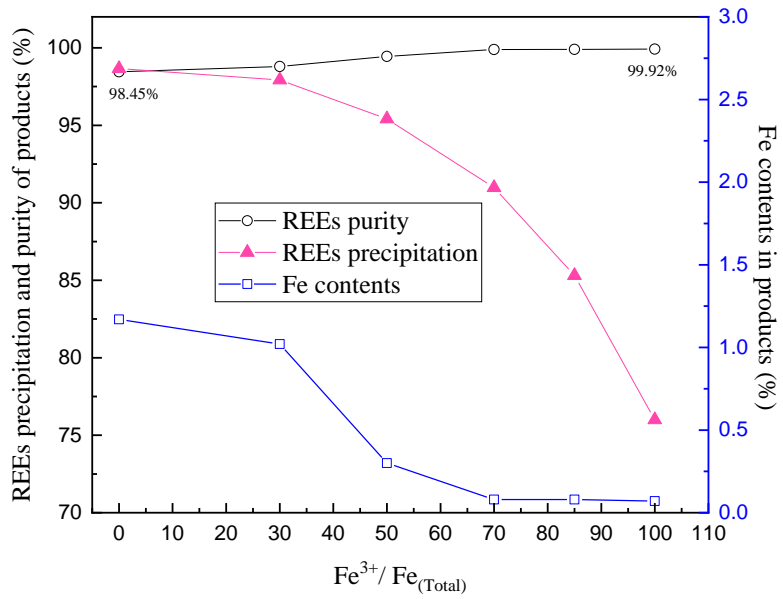


Fig. 3. Effect of  $Fe^{3+}$  ion on the REEs precipitation and purity of oxalate products ( $T = 50\text{ }^{\circ}C$ ;  $t = 60\text{ min}$ ;  $n(\text{oxalic acid})/n(\text{REEs}) = 1.8$ ;  $Nd^{3+} = 20\text{ g/L}$ ;  $Fe_{(total)} = 10\text{ g/L}$ ;  $pH = 0.86$ ).

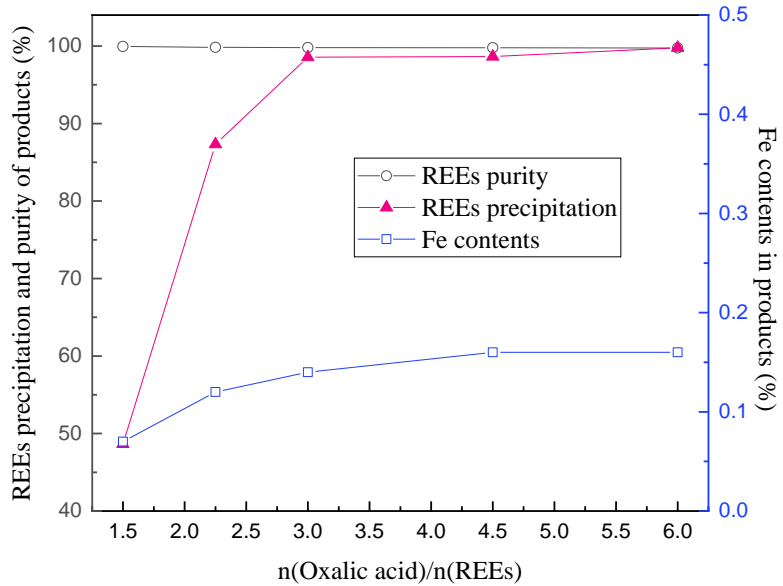


Fig. 4. Effect of oxalic acid on the REEs precipitation and purity of oxalate products ( $T = 50\text{ }^{\circ}C$ ;  $t = 60\text{ min}$ ;  $Nd^{3+} = 20\text{ g/L}$ ;  $Fe^{3+} = 10\text{ g/L}$ ;  $pH = 0.79$ ).

### 3.3. Pressure acid leaching

### 3.3.1 Effect of temperature

The effect of leaching temperature on the recovery of REEs (Nd, Pr, Gd, Ho and Dy), Fe, Co and B from roasted spent magnet powder was investigated with a solution containing 0.6 mol/L HCl. Results presented in Fig. 5 indicate that the leaching of REEs increased from 87.45% to 98.21% as the temperature increased from 120 °C to 180 °C, although a further increase in the temperature from 180 °C to 240 °C resulted in only minor changes in the extraction of REEs. The main reason for the increase is that some of the ferrites produced in roasting, like  $\text{NdFeO}_3$ , can dissolve at temperatures higher than 150 °C (Langová and Matýšek, 2010). XRD results (Fig. 6) show that no  $\text{NdFeO}_3$  could be identified in the leach residues at temperatures higher than 180°C. Moreover, the same findings also indicate that the main Fe-containing phases are akaganeite ( $\text{FeOOH}$ ) and hematite ( $\text{Fe}_2\text{O}_3$ ) at 120 °C, but that almost all Fe is present as hematite after leaching at 180°C (Riveros and Dutrizac, 1997; Cudennec and Lecerf, 2006). This transformation from akaganeite to hematite can reduce the losses of REEs due to adsorption or co-precipitation, as demonstrated by the marked decrease from 8.45% to 3.65% of Fe leaching due to hematite precipitation as temperature increases from 120 °C to 240 °C. Under the same conditions, leaching of B and Co remained almost constant at 96% and 9% over the whole temperature range investigated. The low recovery of cobalt is primarily attributed to the presence of insoluble cobalt ferrite ( $\text{CoFe}_2\text{O}_4$ ) produced in the roasting stage when the roasting temperature was above 700 °C (Radwan and El-Shobaky, 2000).

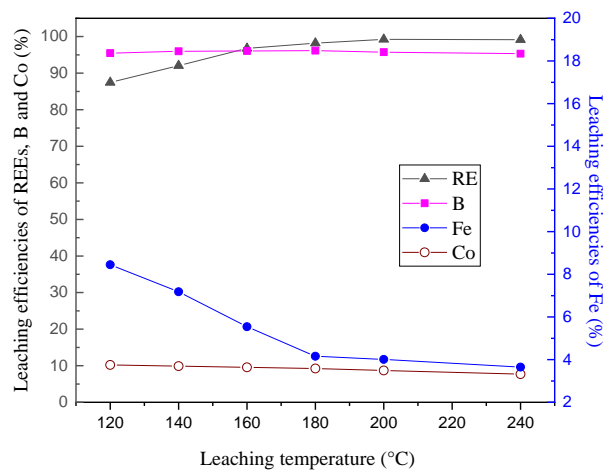
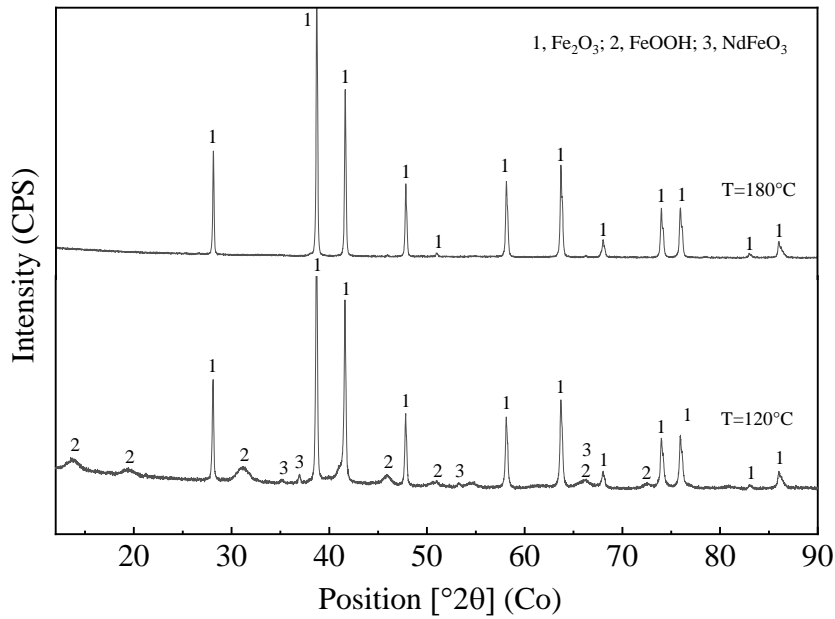


Fig. 5. Effect of leaching temperature on the leaching efficiencies of REEs, B, Fe and Co (HCl = 0.6 mol/L;  $\text{NaNO}_3$  = 0 g/L; t = 120 min; L/S = 10).



23 Fig. 6. X-ray diffraction patterns of the leach residues after leaching at  $T = 120$  and  $180$  °C.

24  
25  
26 **3.3.2. Effect of leaching time**

27  
28 The effect of the leaching time on the leaching of REEs, B, Fe and Co is presented in Fig.  
29 7. These results suggest that the leaching of REEs and B is rapid as approximately 90 % of  
30 the REEs and 75% of the B extracted within the first 30 min, whereas the highest leaching  
31 efficiencies (REEs = 98.2% and B = 96.1%) were reached after 2h. In contrast, although the  
32 leaching of Fe initial increases to 6.1% after 30 min, there is a gradual and continuous  
33 decrease over the remainder of the experiment. The reason for this observed decrease is  
34 ascribed to the increase in akaganeite (FeOOH) and hematite (Fe<sub>2</sub>O<sub>3</sub>) formation with  
35 prolonged time under high temperature and low acidity conditions. When compared with the  
36 metastable ferrihydrite Fe(OH)<sub>3</sub> and akaganeite (FeOOH), the hematite has good  
37 crystallization, poor cation adsorption properties and its solubility,  $K_{sp}$  of  $10^{-43}$  is lower than  
38 either ferrihydrite ( $10^{-39}$ ) or akaganeite ( $10^{-41}$ ) (Cudennec and Lecerf, 2006). Nonetheless, the  
39 transformation from ferrihydrite to hematite is slow, therefore extended leaching times  
40 support the complete removal of Fe, in order to enhance the selective leaching of REEs  
41 (Riveros and Dutrizac, 1997). Under the same conditions, the leaching of cobalt remained  
42 nearly constant at approximately 9% for all leaching times investigated due to the weak  
43 solubility of CoFe<sub>2</sub>O<sub>4</sub> in the low acid solution (Hubli et al., 1997; Tang et al., 2008).  
44  
45  
46  
47  
48  
49  
50  
51  
52  
53  
54  
55  
56  
57  
58  
59  
60  
61  
62  
63  
64  
65

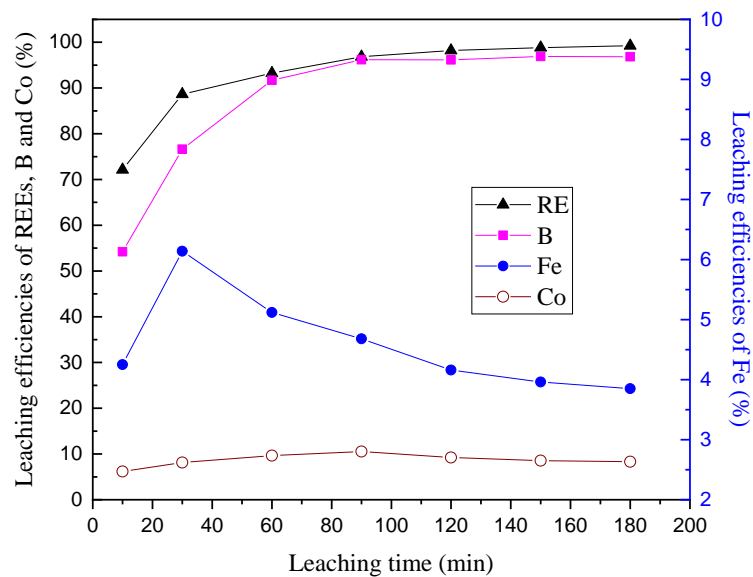


Fig. 7. Effect of leaching time on the leaching efficiencies of REEs, B, Fe and Co ( $T = 180\text{ }^{\circ}\text{C}$ ;  $\text{HCl} = 0.6\text{ mol/L}$ ;  $\text{L/S} = 10$ ;  $\text{NaNO}_3 = 0\text{ g/L}$ ).

### 3.3.3. Effect of hydrochloric acid concentration

The effect of hydrochloric acid concentration on the leaching of REEs (Nd, Pr, Gd, Ho and Dy) and Fe was examined by varying the HCl concentration from 0.3 mol/L to 0.8 mol/L. The results, shown in Fig. 8, indicate that the extraction of REEs and B increased considerably as the hydrochloric acid concentration increased from 0.3 mol/L to 0.6 mol/L - from 46.5 to 98.2% for REEs and from 32.3 to 96.1% for B, respectively. In contrast, further increases in hydrochloric acid concentration from 0.6 mol/L to 0.8 mol/L, only resulted in a minor change to the level of REEs and B extracted. Under the same conditions, the leaching of Fe and Co increased significantly when the initial hydrochloric acid concentration was  $>0.6\text{ mol/L}$ . The XRD results (Fig. 9) of leach residues showed that the REEs ferrite is difficult to dissolve under low acidity conditions, which results in significantly lower levels of REEs and Fe. Conversely, high levels of acidity facilitates the leaching of all the metals from the roasted spent magnet. Irrespectively, the presence of dissolved Fe and Co consumes some oxalic acid during the REEs oxalate precipitation and this can have an adverse effect on the purity of the resultant REEs oxalates (Venkatesan et al., 2018).

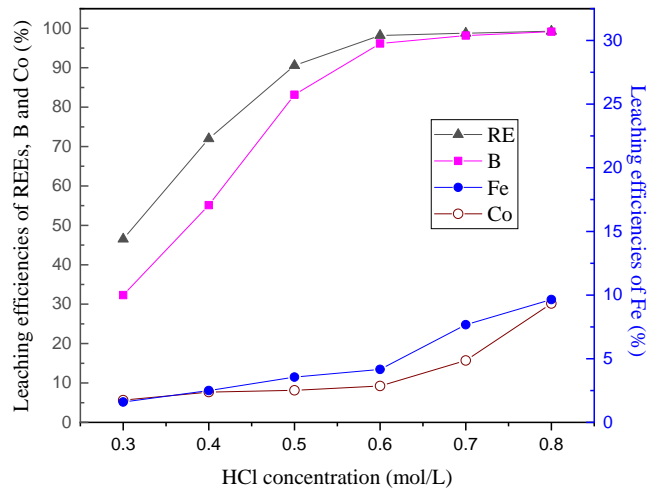


Fig. 8. Effect of HCl on the leaching efficiencies of REEs, B, Fe and Co ( $T = 180^{\circ}\text{C}$ ;  $t = 120$  min;  $L/S = 10$ ;  $\text{NaNO}_3 = 0$  g/L).

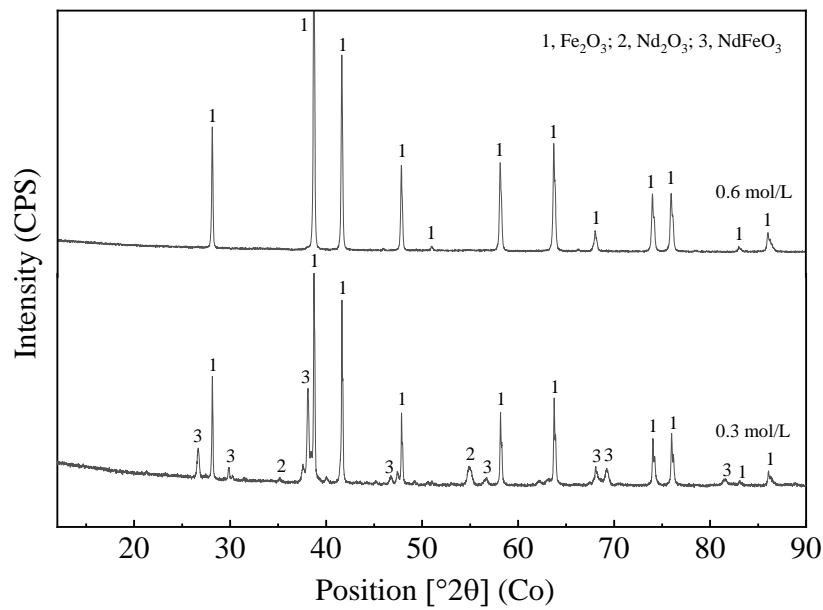
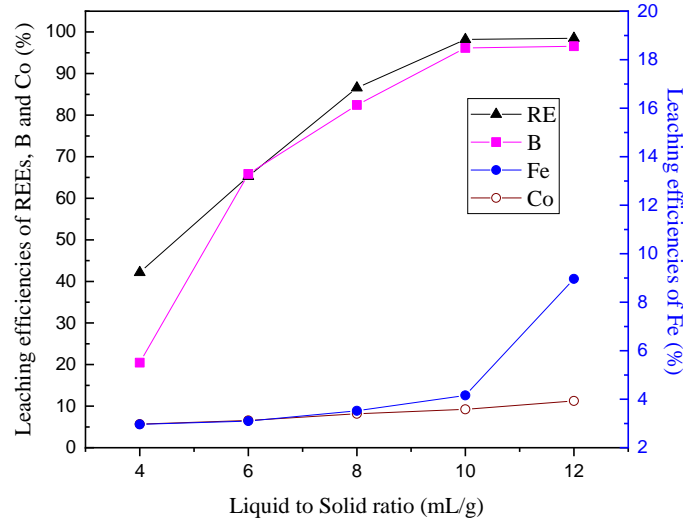


Fig. 9. X-ray diffraction patterns of the leach residues from different acid concentration.

### 3.3.4. Effect of L/S ratio

The leaching results of REEs, B, Fe and Co obtained at different liquid-to-solid (L/S) ratio are displayed in Fig. 10. These results indicate that the leaching of REEs and B increased substantially as L/S increased from 4 to 12, whereas the leaching of Fe remains low until the L/S ratio >10 at which point it starts to increase from 4 to 9%. The increase of Fe leaching results from the higher amount of acid available at the lower pulp density. This increases the

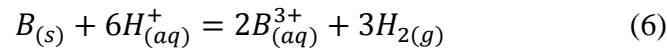
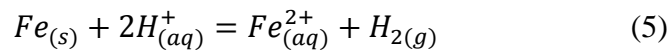
1 Fe dissolution and delays  $Fe^{3+}$  hydrolysis, resulting in the formation of  $Fe_2O_3$  precipitate (Eq.  
 2 (3)). On the other hand, the leaching of Co also increases gradually as the L/S ratio changes  
 3 from 4 to 12, with approximately 11% of Co leached at a L/S ratio of 10. In order to achieve  
 4 the selective separation of REEs and Fe, the optimum L/S ratio is 10, allowing high level of  
 5 REEs (~98%) and B (~96%) leaching with minimal Co or Fe impurities.  
 6  
 7  
 8  
 9



33  
 34 Fig. 10. Effect of liquid to solid (L/S) ratio on the leaching efficiencies of REEs, B, Fe and Co  
 35 ( $T = 180 \text{ }^\circ\text{C}$ ;  $HCl = 0.6 \text{ mol/L}$ ;  $NaNO_3 = 0 \text{ g/L}$ ;  $t = 120 \text{ min}$ ).  
 36  
 37  
 38

### 39 3.3.5. Effect of $NaNO_3$ concentration

40 Phase analysis results of roasted spent magnet samples show that, in addition to the  
 41 presence of  $NdFeO_3$ ,  $Fe_2O_3$  and  $Nd_2O_3$ , the  $Nd_2Fe_{14}B$  phase is still present within the  
 42 materials due to incomplete oxidation of the material. As the REEs and Fe in this metallic  
 43 alloy have high negative standard electrode potentials, they are easily dissolved by  
 44 hydrochloric acid via the following reactions outlined in Eqs. (4) - (6):  
 45  
 46  
 47  
 48  
 49  
 50



After treatment with hydrochloric acid, ferrous ions predominate within the PLS. Fe(II) tends to be stable in solution up to a pH of 6 and Fe(II) oxalates are highly insoluble, whereas in contrast, Fe(III) precipitates at a pH around 2-3 and Fe(III) oxalates are highly soluble. Therefore, in order to achieve a good separation of REEs and Fe, the selective oxidation of Fe(II) is necessary and NaNO<sub>3</sub> was selected as an oxidant in order to mitigate the iron dissolution.

The effect of sodium nitrate addition on the leaching of REEs, B, Fe and Co were examined with a total pressure 0.62 MPa, an HCl concentration of 0.6 mol/L and an L/S ratio of 10 at 180 °C for 2 h (Fig. 11). As can be observed, the leaching of Fe shows a continuous decrease - from approx. 4% to nearly 0% - as NaNO<sub>3</sub> concentration is increased from 0 g/L to 2 g/L. At the same time the leaching of REEs, B and Co remained almost constant at approximately 99%, 97% and 7%, respectively. This appreciable decrease in the level of Fe leaching can be ascribed to the oxidation of the dissolved Fe(II) ion (Eq. (7)) in the solution due to the introduction of the NaNO<sub>3</sub> oxidant.

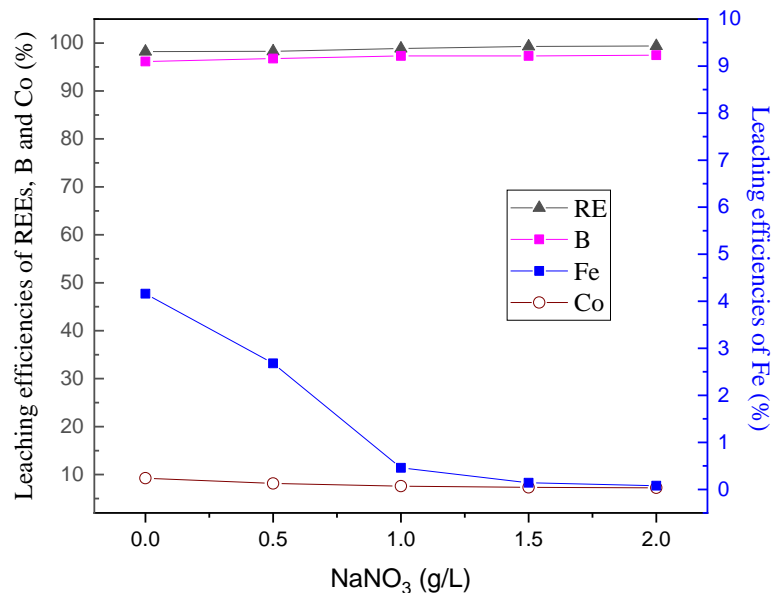
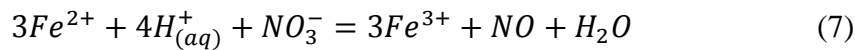


Fig. 11. Effect of NaNO<sub>3</sub> concentration on the leaching of REEs, B, Fe and Co ( $T = 180\text{ }^{\circ}\text{C}$ ;  $t = 120\text{ min}$ ;  $\text{HCl} = 0.6\text{ mol/L}$ ;  $\text{L/S} = 10$ ).

Based on the results shown in Fig. 11, the most suitable leaching conditions for the roasted spent magnet powder were determined to be HCl concentration of 0.6 mol/L, NaNO<sub>3</sub>

concentration of 2 g/L, L/S ratio of 10, temperature of 180 °C and a total leaching time of 2 h. Under these conditions it was determined that > 98% REEs and < 0.1% Fe could be leached to a solution (pH 2.1), to produce the following approximate PLS composition: 19.01 g/L Nd, 4.66 g/L Pr, 1.30 g/L Dy, 0.14 g/L Gd, 0.61 g/L Ho, 0.70 g/L B with trace amounts of Fe (0.04 g/L) and Co (0.05 g/L). Additionally, the XRD results (Fig. 9) showed that the dominating phase in the leach residue was hematite (Fe<sub>2</sub>O<sub>3</sub>).

### 3.4. REEs oxalate precipitation

The effective separation of REEs and Fe can be achieved by hydrochloric acid pressure leaching as this not only helps avoid any adverse impact of impurities on product quality, but also reduces oxalic acid consumption. The effect of oxalic acid levels on the precipitation of REEs in Fe-free solution was investigated in more detail with a reaction temperature of 50 °C, initial pH = 2.2 and 30 min reaction time. As shown in Fig. 12, all of the Nd, Gd, Pr, Dy and Ho were precipitated at a  $n(\text{oxalic acid})/n(\text{REEs})$  of 1.1. When compared with high concentration iron solution (Fig. 3 and 4), the consumption of oxalic acid is significantly reduced, however when taking into account the reusability of the aqueous solution for a new leaching experiment, a value of  $n(\text{oxalic acid})/n(\text{REEs}) = 1$  was selected. At this value, 99.9% of REEs can be recovered with a REEs oxalates product purity > 99.9% and almost all the oxalic acid is consumed during the precipitation process. Subsequent XRD analysis (Fig.13a) showed that the main phases with the products are hydrated REEs oxalates, with generic formula of RE<sub>2</sub>(C<sub>2</sub>O<sub>4</sub>)<sub>3</sub>·4.5 H<sub>2</sub>O. These oxalates have an excellent crystallinity and a particle size within the range of 1-5 μm (Fig.13 b).

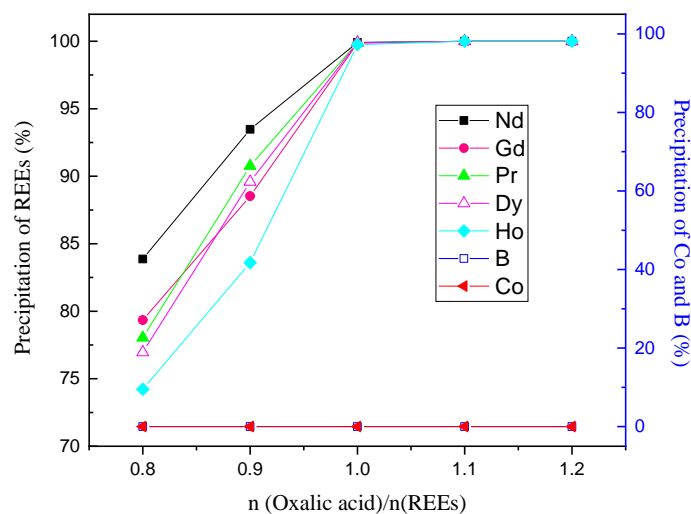


Fig. 12. Effect of the amount oxalic acid on the precipitation of REEs, Co and B

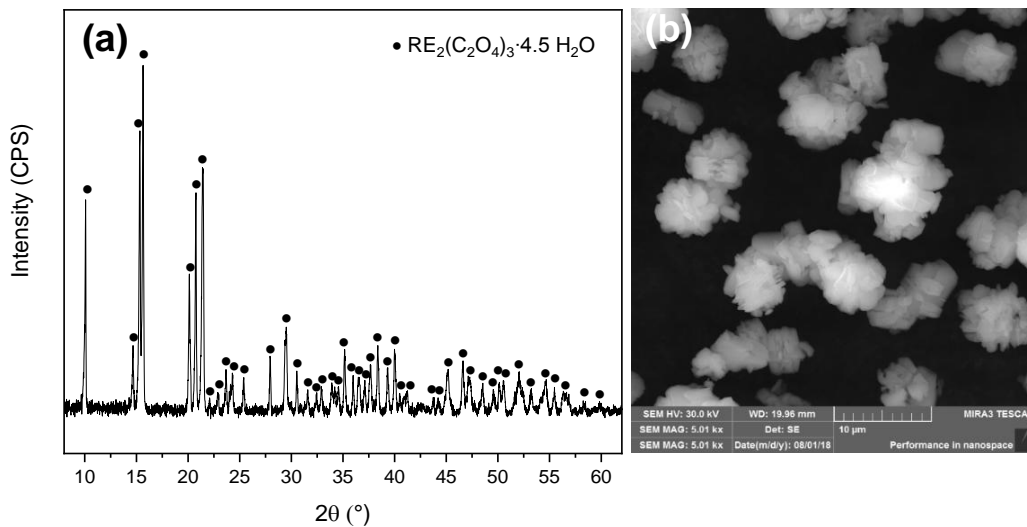


Fig. 13. Characterization of REEs oxalate precipitation with (a) XRD and (b) SEM.

### 3.5. Separation of boron from the REEs-free solution

After REEs precipitation, the concentration of B and Co in the REEs-free solution were in the order of 680 mg/L and 50 mg/L (pH 0.45), with the boron mainly present as  $H_3BO_3$  (Wolska and Brijak, 2013). As the B concentration is low, it is difficult to recover economically or efficiently with classical processes like co-precipitation, ion exchange and solvent extraction; therefore, it is necessary to enrich the B firstly by multiple leaching cycles. In this work, the concentration of B and Co reached levels of 3.30 g/L and 0.24 g/L after five leaching cycles. A solvent extraction method was carried out using an extractant mixture that comprised of 30% (v/v) 2-ethyl-1,3-hexanediol (EHD), 70% (v/v) sulfonated kerosene for the B recovery. Results showed that boron extraction attained was 99.5% with a three-stage counter current extraction at an O/A ratio of 1:2 at 30 °C for 10 min. A boron stripping ratio of > 91.2% was achieved when the loaded organic phase was removed by NaOH (0.1mol/L) for 15 min at 30 °C with an O/A ratio of 1:2. This recovery was enhanced further by use of a three-stage counter current stripping, which resulted in B stripping ratios >99.6% and a stripping liquor containing 3.0 g/L of boron.

After boron recovery, the  $Na_2S$  precipitation method (Vemic et al., 2016; Elwert et al., 2013) was adopted to remove the cobalt as CoS from the boron-free solution. Based on the results of the pretreatment, pressure leaching and boron solvent extraction outlined, a process flow sheet that allows for the recovery of REEs, Fe, B and Co was developed (Fig. 14). Compared with existing methodologies, this new process has the potential to improve

significantly the recovery of valuable metals, and is more environmentally friendly due to the reduced levels of boron-containing wastewater and required amounts of oxalic acid.

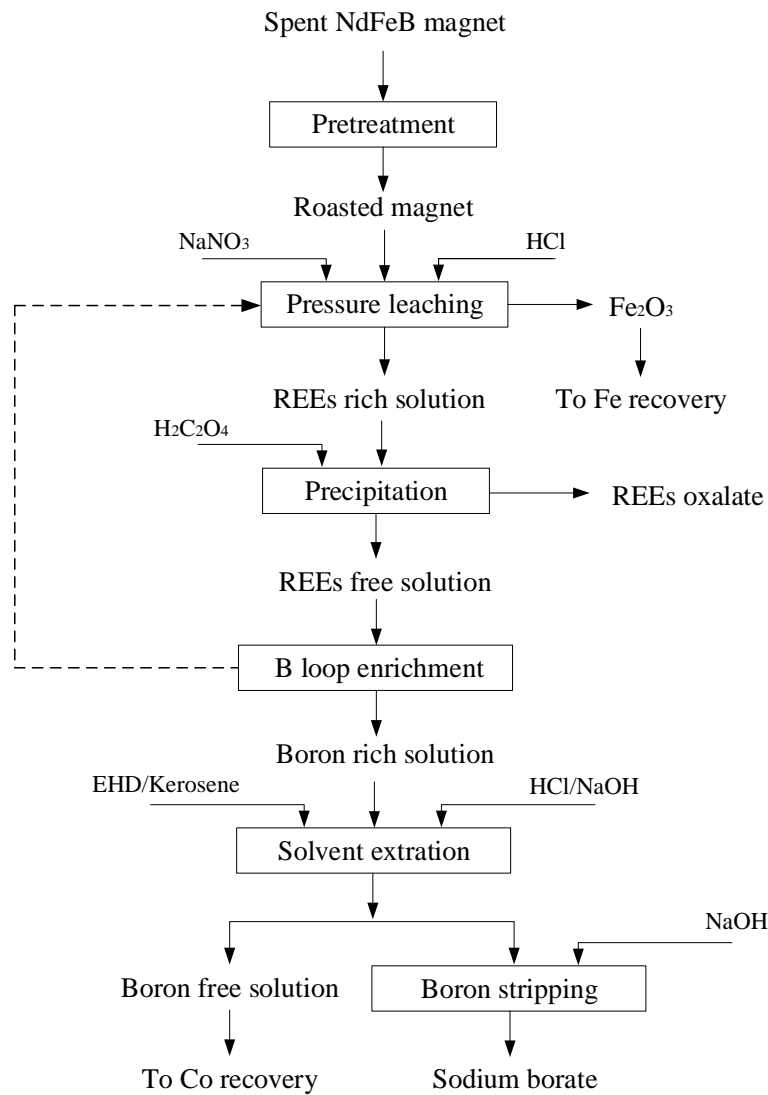


Fig. 14. Proposed flowsheet for recovery of REEs, Fe, B and Co from spent Nd-Fe-B magnets.

#### 4. Conclusions

This research outlines a novel method to separate the REEs from spent Nd-Fe-B magnet materials by a combined pretreatment, REEs oxalate precipitation, boron solvent extraction and cobalt precipitation process. In particular, optimization of the selective leaching of REEs vs. Fe is highlighted as this decreases both solution purification operational costs and minimizes oxalate consumption in REEs recovery stage.

1 For the pretreatment stage, a temperature of 800 °C was selected to avoid excessive  
2 oxidation, which leads to unsatisfactory REEs extraction, and insufficient roasting that results  
3 in poor selectivity separation of REEs and Fe. Additionally, it was found that the existence of  
4 Fe(II) in the oxalate solution had a negative impact on REEs product purity, and ferric ions  
5 Fe(III) result in increased levels of oxalic acid consumption due to strong complexation  
6 between oxalate and ferric ions.-  
7  
8  
9

10 In the pressure-leaching step, increased temperature and prolonged leaching times can be  
11 both utilized to achieve the effective removal of Fe. Moreover, the use of NaNO<sub>3</sub> as an  
12 oxidant can radically reduce the level of Fe dissolution to < 0.1%, whilst the leaching  
13 efficiencies of Nd, Pr, Dy, Gd and Ho were maintained at > 98%. This clearly demonstrates  
14 that REEs and Fe can be leached selectively from roasted spent Nd-Fe-B magnet materials.  
15  
16  
17  
18  
19

20 After leaching, >99% of REEs can be precipitated by oxalic acid at the value  $n(\text{oxalic}$   
21  $\text{acid})/n(\text{REEs})$  of 1. Finally, 99.5% of boron is recovered by an extractant mixture composed  
22 of 30% (v/v) (EHD) and 70% (v/v) sulfonated kerosene with a three-stage counter current  
23 extraction, followed by NaOH stripping. These findings demonstrate that high recoveries of  
24 REEs, Fe and B are achievable with roasting pretreatment and hydrochloric acid pressure  
25 leaching followed oxalate precipitation and boron recovery.  
26  
27  
28  
29  
30

31 The existing technical challenges such as difficulties of rare earth elements (REEs) and Fe  
32 separation, low products purity and large-scale generation of boron wastewater in the exiting  
33 processes have been well solved by this new developed process.  
34  
35  
36  
37

### 38 **Acknowledgements**

39 The authors acknowledge HYMAG project (SL/84/04.03.00.0400/2017) funded by the  
40 Regional Council of Satakunta, AIKO funding. This paper also made use of the Academy of  
41 Finland's RawMatTERS Finland Infrastructure (RAMI) based at Aalto University. The  
42 authors also acknowledge the financial support from the National Nature Science Foundation  
43 of China (No.51804141) as well as the Science and Technology Project of the Education  
44 Department of Jiangxi Province (GJJ170533).  
45  
46  
47  
48  
49  
50  
51

### 52 **References**

53  
54  
55  
56  
57 Bandara, H. M. D., Field K. D., Emmert, M. H., 2016. Rare earth recovery from end-of-  
58 life motors employing green chemistry design principles. Green Chem. 18, 753-759.  
59  
60  
61  
62  
63  
64  
65

1 Battsengel, A., Batnasan, A., Narankhuu, A., Haga, K., Watanabe, Y., Shibayama, A.,  
2 2018. Recovery of light and heavy rare earth elements from apatite ore using sulphuric acid  
3 leaching, solvent extraction and precipitation. *Hydrometallurgy* 179, 100-109.

4 Beltrami, D., Deblonde, G. J. P., Bélair, S., Weigel, V., 2015. Recovery of yttrium and  
5 lanthanides from sulfate solutions with high concentration of iron and low rare earth content.  
6 *Hydrometallurgy* 157, 356–362.

7  
8 Binnemans, K., Jones, P. T., 2015. Rare Earths and the Balance Problem. *J. Sustain.*  
9 *Metallurgy* 1 (1), 29-38.

10  
11 Binnemans, K., Jones, P.T., 2014. Perspectives for the recovery of rare earths from end-of-  
12 life fluorescent lamps. *J. Rare Earths* 32, 195–200.

13  
14 Cudennec, Y., Lecerf, A., 2006. The transformation of ferrihydrite into goethite or  
15 hematite, revisited. *Journal of Solid State Chemistry* 179, 716–722.

16  
17 Du, X.Y., Graedel, T. E., 2011. Global In-Use Stocks of the Rare Earth Elements: A First  
18 Estimate. *Environmental Science and Technology* 45, 4096–4101.

19  
20 Elwert, T., Goldmann, D., Schmidt, F., Stollmaier R., 2013. Hydrometallurgical recycling  
21 of sintered NdFeB magnets. *World Metall* 66(4), 209-219.

22  
23 Firdaus, M., Rhamdhani, M. A., Rankin, W. J., Pownceby, M., Webster, N. A. S.,  
24 D'Angelo, A. M., Kathie McGregor, K., 2018. High temperature oxidation of rare earth  
25 permanent magnets. Part 1-Microstructure evolution and general mechanism. *Corrosion*  
26 *Science* 133, 374-385.

27  
28 Hoogerstraete, V., Blanpain, B., Gerven, T.V., Binnemans, K., 2014. From NdFeB  
29 magnets towards the rare-earth oxides: a recycling process consuming only oxalic acid. *RSC*  
30 *Adv.* 4, 64099–64111.

31  
32 Horikawa, T., Miura, K., Itoh, M., Machida, K.I., 2006. Effective recycling for Nd–Fe–B  
33 sintered magnet scraps. *Journal of Alloys and Compounds* 408-412, 1386-1390.

34  
35 Hubli, R.C., Mitra, J., Suri, A.K., 1997. Reduction-dissolution of cobalt oxide in acid  
36 media: a kinetic study, *Hydrometallurgy* 44, 25-114.

37  
38 Itoh, M., Miura, K., Machida, K., 2008. Novel rare earth recovery process on Nd–Fe–B  
39 magnet scrap by selective chlorination using  $\text{NH}_4\text{Cl}$ . *J Alloys Comp* 477, 484–487.

40  
41 Jha, M. K., Kumari A., Panda R., Kumar, J. R., Yoo, K., Lee, J.Y., 2016. Review on  
42 hydrometallurgical recovery of rare earth metals. *Hydrometallurgy* 161, 77–101.

43  
44 Koyama, K., Kitajima, A., Tanaka, M., 2009. Selective leaching of rare-earth elements  
45 from an Nd-Fe-B magnet. *Kidorui (Rare Earths)* 54, 36–37.

46  
47 Kruse, S., Raulf, K., Pretz, T., Friedrich, B., 2017. Influencing factors on the melting  
48 characteristics of NdFeB-Based production wastes for the recovery of rare earth compounds.  
49 *Journal of Sustainable Metallurgy* 3, 168 – 178.

50  
51 Kumari, A., Sinha, M. K., Pramanik, S., Sahu, S. K., 2018. Recovery of rare earths from  
52 spent NdFeB magnets of wind turbine: Leaching and kinetic aspects. *Waste Management* 75,  
53 486–498.

54  
55 Langová, Š., Matýsek, D., 2010. Zinc recovery from steel-making wastes by acid pressure  
56 leaching and hematite precipitation. *Hydrometallurgy* 101, 171–173.

57  
58  
59  
60  
61  
62  
63  
64  
65

1 Lee, C.H., Chen, Y.J., Liao, C.H., Popuri, S.R., Tsai, S.L., Hung, C.E., 2013. Selective  
2 leaching process for neodymium recovery from scrap Nd-Fe-B magnet. *Metall. Mater. Trans.*  
3 *A 44*, 5825–5833.

4 Lee, J. C., Kim, W. B., Jeong, J., Yoon, I. J., 1998. Extraction of neodymium from Nd-Fe-  
5 B magnet scraps by sulfuric acid. *J Korean Inst Met Mater* 36(6), 967–972

6  
7 Liu, F. P., Liu, Z. H., Li, Y. H., Wilson, B. P., Lundström, M., 2017. Extraction of Ga and  
8 Ge from zinc refinery residues in  $H_2C_2O_4$  solutions containing  $H_2O_2$ . *International Journal of*  
9 *Mineral Processing* 163, 14 - 23.

10  
11 Lyman, J.W., Palmer, G.R., 1993. Recycling of rare earths and iron from NdFeB magnet  
12 scrap. *High Temp. Mater. Proc.* 11, 175–187.

13  
14 Morgan, B.; Lahav, O., 2007. The effect of pH on the kinetics of spontaneous Fe(II)  
15 oxidation by  $O_2$  in aqueous solution--basic principles and a simple heuristic description.  
16 *Chemosphere* 68 (11), 2080-4.

17  
18 Murase, K., Machida, K., Adachi, G., 1995. Recovery of rare metals from scrap of rare  
19 earth inter-metallic material by chemical vapor transport. *J Alloys Comp* 217, 218–225.

20  
21 Önal M. A. R., Borra, C. R., Guo, M. X., Blanpain, B., Gerven, T.V., 2017.  
22 Hydrometallurgical recycling of NdFeB magnets: Complete leaching, iron removal and  
23 electrolysis. *Journal of rare earths*, 35(5): 574-583.

24  
25 Önal, M. A. R., Borra, C. R., Guo, M. X., Blanpain, B., Gerven, T. V., 2015. Recycling of  
26 NdFeB Magnets Using Sulfation, Selective Roasting, and Water Leaching. *J. Sustain. Metall.*  
27 1, 199–215.

28  
29 Önal, M.A.R., Aktan, E., Borra, C.R., Blanpain, B., Gerven, T.V., Guo, M.X., 2017.  
30 Recycling of NdFeB magnets using nitration, calcination and water leaching for REE  
31 recovery. *Hydrometallurgy* 167, 115-123.

32  
33 Panayotova, M., Panayotov, V., 2012. Review of methods for the rare earth metals  
34 recycling. *Annual of the University of Mining and Geology, St. Ivan Rilski, Min. Miner.*  
35 *Process.* 55, 142–147.

36  
37 Petranikova, M., Herdzik-Koniecko, I., Steenari, B.M., Ekberg, C., 2017.  
38 Hydrometallurgical processes for recovery of valuable and critical metals from spent car  
39 NiMH batteries optimized in a pilot plant scale. *Hydrometallurgy*, 171: 128-141.

40  
41 Rabatho, J. P., Tongamp, W., Takasaki, Y., Haga, K., Shibayama, A., 2013. Recovery of  
42 Nd and Dy from rare earth magnetic waste sludge by hydrometallurgical process. *J Mater*  
43 *Cycles Waste Manag* 15, 171–178.

44  
45 Radwan, N.R.E., EI-Shobaky, 2000. Solid–solid interactions between ferric and cobalt  
46 oxides as influenced by  $Al_2O_3$ -doping. *Thermochimica Acta*, 360(2): 147-156.

47  
48 Riveros, P. A., Dutrizac, J. E., 1997. The precipitation of hematite from ferric chloride  
49 media. *Hydrometallurgy* 46, 85-104.

50  
51 Saito, T., Sato, H., Ozawa, S., Yu J., Motegi T., 2003. The extraction of Nd from waste  
52 Nd–Fe–B alloys by the glass slag method. *J Alloys Comp* 353, 189 –193.

53  
54  
55  
56  
57  
58  
59  
60  
61  
62  
63  
64  
65

1 Sasaki, K., Qiu, X., Hosomomi, Y., Moriyama, S., Hirajima, T., 2013. Effect of natural  
2 dolomite calcination temperature on sorption of borate onto calcined products. *Microporous*  
3 *Mesoporous Mater.* 171, 1-8.

4 Sun, M., Hu, X., Peng, L., Fu, P., Ding, W., Peng, Y., 2015. On the production of Mg-Nd  
5 master alloy from NdFeB magnet scraps. *J. Mater. Proc.* 218, 57-61.

6  
7 Tagliabue, M., Reverberi, A. P., Bagatin, R., 2014. Boron removal from water: needs,  
8 challenges and perspectives. *Journal of Cleaner Production* 77, 56-64.

9  
10 Tang, C. W., Wang, C.B., Chien, S. H., 2008. Characterization of cobalt oxides studied by  
11 FT-IR, Raman, TPR and TG-MS. *Thermochimica Acta* 473(1-2): 68-73.

12 Tu, K.L., Nghiem, L.D., Chivas, A.R., 2010. Boron removal by reverse osmosis  
13 membranes in seawater desalination applications. *Sep. Purif. Technol.* 75, 87-101.

14  
15 Tunsu, 2018. Hydrometallurgy in the recycling of spent NdFeB permanent magnets,  
16 *Waste Electrical and Electronic Equipment Recycling* 8, 175-211.

17  
18 Vemic, M., Bordas, F., Comte, S., Guibaud, G., Lens P. N. L., Hullebusch, E. D. V., 2016.  
19 Recovery of molybdenum, nickel and cobalt by precipitation from the acidic leachate of a  
20 mineral sludge. *Environmental Technology* 37 (17), 2231-2242,

21  
22 Venkatesan, P., Sun, Z., Sietsma, J., Yang, Y.Y., 2018. An environmentally friendly  
23 electro-oxidative approach to recover valuable elements from NdFeB magnet waste.  
24 *Separation and Purification Technology* 191, 384-391.

25  
26 Wolska, J., Brijak, M., 2013. Methods for boron removal from aqueous solutions. A  
27 review. *Desalination* 310, 18-24

28  
29 Xu, Y., Jiang, J.Q., 2008. Technologies for boron removal. *Ind. Eng. Chem. Res.* 47, 16-  
30 24.

31  
32 Yang, Y. X., Walton, A., Sheridan, A., Guth, K., Gauß, R., Gutfleisch, O., Buchert, M.,  
33 Steenari, B. M., Gerven, T. V., Jones, P. T., Binnemans, K., 2017. REE Recovery from End-  
34 of-Life NdFeB Permanent Magnet Scrap: A Critical Review, *J. Sustain. Metall.* 3:122-149.

35  
36 Zhou, X., Tian, Y.L., Yu, H.Y., Zhang, H., Zhong, X.C., Liu, Z.W., 2019. Synthesis of  
37 hard magnetic NdFeB composite particles by recycling the waste using microwave assisted  
38 auto-combustion and reduction method. *Waste Management* 87, 645-651.

39  
40  
41  
42  
43  
44  
45  
46  
47  
48  
49  
50  
51  
52  
53  
54  
55  
56  
57  
58  
59  
60  
61  
62  
63  
64  
65

### **Research Highlights**

- (1) Oxidative roasting and adding  $\text{NaNO}_3$  both can promote the selective separation of REEs.
- (2)  $> 99\%$  of REEs and  $< 0.01\%$  of Fe could be extracted by pressure leaching process.
- (3) The removal of Fe enhances REEs recovery and minimizes the oxalic acid consumption.
- (4) Boron can be effectively enriched and recovered by solvent extraction process.
- (5) A new process for the recovery of REEs, Fe and B from spent magnet was proposed